Journal of Building Engineering 40 (2021) 102378

Contents lists available at ScienceDirect

Journal of Building Engineering

journal homepage: http://www.elsevier.com/locate/jobe

Assessment of thermal comfort indices in an open air-conditioned stadium in hot and arid environment

Saud Ghani [a], Ahmed Osama Mahgoub [a,*], Foteini Bakochristou [a], Esmail A. ElBialy [b]

[a] Department of Mechanical and Industrial Engineering, Qatar University, P.O. Box 2713, Doha, Qatar
[b] Faculty of Engineering, Cairo University, 12613, Giza, Egypt

ARTICLE INFO

Keywords:
Thermal comfort
Outdoor environment
Thermal comfort indices
Thermal comfort questionnaire
Air-conditioned stadiums
CFD

ABSTRACT

Thermal comfort indices are vital tools when assessing outdoor thermal comfort in hot and arid environments. Selecting a representative thermal comfort index for outdoor environments is challenging. This paper presents a comparative study of the suitability of seven different thermal comfort indices, namely PMV, discomfort index, cooling power index, Humidex, WBGT, SET, and UTCI in assessing outdoor thermal comfort. The thermal comfort indices were compared to the thermal sensation vote (TSV) obtained from a thermal comfort questionnaire of spectators seated in a semi-open air-conditioned stadium. Seated in six different zones, a total of 532 spectators participated in an online questionnaire. The results of the survey indicated high levels of climate acceptability, with small variations among the stadium zones and between genders. Almost 40% of the spectators reported feeling "*cool*", while 28% of the spectators were feeling "*slightly cool*" and 21% reported a "*neutral*" thermal perception. Hence, CFD simulations were used to predict the values of the seven thermal comfort indices. The thermal comfort indices' values, obtained from the CFD simulations, were compared to their counterparts obtained from the questionnaire. The WBGT index showed good agreement to the actual questionnaire data with an average difference of 8.8%. The other six indices yielded an average range of difference of (15%–46%). The WBGT index deemed the most suitable to assess outdoor thermal comfort for hot and arid regions, followed by the UTCI and the SET indices, with average differences of 14% and 15%, respectively. The CPI index deemed not suitable for hot and arid regions compared to other indices.

1. Introduction

The thermal environment affects the human's body system which reacts according to the basic laws of thermodynamics [1]. Comfortable and healthy outdoor microclimates are beneficial to sustainable urban development and public health [2]. Providing thermal comfort for outdoor environments is highly sensitive to the prevailing meteorological conditions, where typical engineering climate control solutions may prove to be inadequate [3]. Thermal comfort indices are vital tools when assessing outdoor thermal comfort in hot and arid environments. In previous studies, various thermal comfort indices were introduced. However, selecting a representative thermal comfort index is challenging, especially for outdoor thermal comfort evaluation in hot and arid environment.

1.1. Thermal comfort in outdoor environments

As people spend the majority of their lifetime indoors, outdoor thermal comfort receives less attention than indoor thermal comfort. However, outdoor thermal comfort is becoming an important aspect of the recreational and entertainment business. Currently, more people are actively pursuing healthy lifestyle and participation in outdoor activities, such as outdoor athletic events and outdoor dining. The current thermal comfort standards for indoor human activities are assessing thermally static and uniformly controlled environments. Outdoor thermal conditions are frequently changing in time and space [4] and are dynamic and mutable. Thus, it is inherently difficult to assess outdoor thermal comfort using the indoor standards and guidelines [5]. To offer better outdoor human thermal comfort, a thorough understanding of urban climatology and landscape architecture is essential [6]. The challenge in assessing human outdoor thermal comfort lies on the fact that the human body energy balance equation includes parameters that are mainly influenced by the weather. The respiration convective flux

* Corresponding author.
E-mail address: ahmed.mahgoub@qu.edu.qa (A.O. Mahgoub).

https://doi.org/10.1016/j.jobe.2021.102378
Received 22 September 2020; Received in revised form 2 February 2021; Accepted 2 March 2021
Available online 6 March 2021

Abbreviations

ASHRAE	American society of heating, refrigerating and air-conditioning engineers
CFD	Computational fluid dynamics
CI	Cooling index
CPI	Cooling power index
DI	Discomfort index
ET	Effective temperature
FIFA	Féderationé Internationalé de Football Association
MCV	Mean comfort vote
mTSV	Mean thermal sensation vote
PET	Physiological effective temperature
PT	Physiological temperature
PMV	Predicted mean vote
RANS	Reynolds-averaged Navier Stokes
SET	Standard effective temperature ($^{\circ}C$)
TSV	Thermal sensation vote
UDF	User-defined function
UTCI	Universal temperature climatic index
WBGT	Wet bulb globe temperature
e	The base of the natural logarithm = 2.71828
h_s	Standard heat transfer coefficient ($W/m^{2\cdot\circ}C$)
$h_{s,e}$	Standard evaporative heat transfer coefficient (W/m^2.kPa)
J	Diffusion flux due to the gradient of species concentration
k	Turbulent kinetic energy (m^2/s^2)
L	Thermal load on the body (W/m^2)
M	Metabolic rate of human body (W/m^2)
p	Pressure (Pa)
p_{SET}	Saturated water vapor pressure at SET (kPa)
$p_{s,sk}$	Water vapor pressure at skin, assumed to be that of saturated water vapor at t_{sk} (kPa)
p_v	Atmospheric pressure of water vapor (mm Hg)
RH%	Relative humidity (%)
T	Temperature (K)
T_{db}	Dry bulb temperature ($^{\circ}C$)
t_{sk}	Skin temperature ($^{\circ}C$)
T_w	Wet bulb temperature ($^{\circ}C$)
T_G	Black globe temperature ($^{\circ}C$)
u	Velocity vector (m/s)
V	Air velocity magnitude (m/s)
w	Fraction of the wetted skin surface
ε	Turbulent dissipation rate (m^2/s^3)
κ	Thermal conductivity of air (W/mK)
ν	Kinematic viscosity of air (m^2/s)
ρ	Density of air (kg/m^3)
φ	Species concentration (kg/kg)
∇	Gradient operator $\left(\frac{\partial}{\partial x}\mathbf{i}+\frac{\partial}{\partial y}\mathbf{j}+\frac{\partial}{\partial z}\mathbf{k}\right)$

and heat flux are temperature dependent, while the latent heat flux diffusing through the human skin and the heat flux due to evaporation of sweat are affected by the ambient humidity levels [7]. In addition, the thermal sensation of the individual is affected by the personal climate background [8], their gender [4] and clothes that affect the skin humidity and define levels of discomfort [9]. The prevailing air velocity also affects the human thermal comfort. Different comfort levels are obtained at different wind speeds [10]. Human adaption to the prevailing climates with special clothing suitable for different conditions, results into multiple clothing insulation indices [11].

Recently, interest in thermally controlling the outdoor environments had increased. Thermal comfort in outdoor environments can be enhanced by utilizing of shading, water features, cool surfaces and vegetation [12–15]. For outdoor thermal comfort assessment, the physiological effective temperature (PET) and the universal thermal climate index UTCI are usually used. The predicted mean vote (PMV), which was mainly proposed to be used indoors, had also been used to investigate thermal comfort in outdoor environments [13,16]. Thermal comfort surveys are performed to obtain the thermal sensation vote (TSV), which is used for indoor and outdoor thermal comfort assessment [17,18]. For thermal comfort assessment in an outdoor air-conditioned area (FANZONE), Ghani et al. (2017) [8] compared five different thermal indices. In their study, with the except ion of the WBGT index, all the other four thermal indices underestimated the thermal comfort levels of the mean comfort vote (MCV) obtained from a thermal survey.

Open roof stadiums are regarded as outdoor spaces. The stadium thermal climate is mainly affected by the prevailing environmental conditions and the indoor climate control from the air conditioning units [19]. In stadiums, thermal comfort assessment is essential for both the players in the field and the spectators in the tiers [20]. Evaluation of heat stress of players inside the stadium's field of play is essential in deciding whether cooling breaks should be included [21]. The assessment of thermal comfort for spectators is essential for all outdoor sporting activities and is not limited to football games in stadiums, and an example for such activities was the Olympic marathon [22].

1.2. Climatic thermal comfort indices

In outdoor environments, human thermal comfort depends on the prevailing environmental factors such as the ambient temperature, humidity, wind speed and solar radiation [23,24]. These parameters are considered as the thermal standards that can assess the state of comfort of the individual for given weather conditions [25]. The investigated indices include various parameters, that are either measured directly or given by international standards [26,27]. For outdoor thermal comfort assessments, adopting a solely heat balance analysis of the individual is not recommended. As thermal preferences are additionally influenced by experience (thermal-weather background) of the participants and present seasonal fluctuations [28]. For example, individuals acclimatized in warmer environments present lower metabolic rates [29].

Controlling outdoor environments is more challenging than indoor environments. For outdoor environments, there is a need for global thermal comfort assessment compared to pointwise measurements which are typically used in indoor environments. Mahgoub et al. (2020) performed global evaluation of WBGT and SET indices in stadiums using a newly proposed methodology. The results obtained by the proposed methodology yielded an error of 2% compared to point-wise evaluation [20].

Several studies addressed the evaluation of outdoor thermal comfort in different regions using various thermal comfort indices. Using the PET index, Wang et al. (2018) evaluated the effect of green spaces on urban environment thermal comfort [18]. It was found that a high density of trees does always lead to better thermal sensation. Fong et al. (2019) proposed a holistic approach for future outdoor thermal comfort evaluation in tropical regions [30]. Using the PET index, Deng and Wong (2020) investigated the impact of canyon geometries in urban business districts on outdoor thermal comfort. The study found a correlation between canyon geometry and the thermal comfort [31]. Berardi and Graham (2020) used UTCI to examine the effect of street trees, cool roofs and photovoltaics roofs on the outdoor thermal comfort [32]. The study showed that the UTCI increased by about 0.5°C when using photovoltaics roofs. Using the temperature humidity index (THI), Balogun and Daramola (2019) assessed the effect different urban configurations on

outdoor thermal comfort [33]. Binarti et al. (2020) presented a review of indices used for outdoor thermal comfort in hot and humid regions. The study provided recommendations regarding the neutral ranges of PET, SET and UTCI indices in these regions [34]. Elnabawi and Hamza (2019) suggested a framework for the evaluation of the relationship between thermal comfort assessment and social behavior of population in outdoor environments [35]. Cheung and Jim (2019) proposed a 1-h acceptability level for enhanced outdoor thermal comfort evaluation [36]. The results from the proposed method were compared to the PET and UTCI indices. Matallah et al. (2020) used the PET index to evaluate outdoor thermal comfort in Saharan oases [37]. It was found that oases did not have an apparent effect on thermal comfort. Nazarian et al. (2019) proposed the use of outdoor thermal comfort as performance metrics for climate conscious urban design [38]. Sharmin et al. (2019) conducted thermal surveys to evaluate the thermal sensation votes (TSV) as a measure of outdoor thermal comfort in the tropical city of Dhaka [39]. Potchter et al. (2018) [16] reviewed the methods for assessing human thermal perception in outdoor environments. In their review, it was stated that although there have been 165 thermal indices, only four are widely used for outdoor thermal comfort assessment. Namely, the physiological effective temperature (PET), PMV, UTCI and SET.

Guided by the published research on evaluation of thermal comfort in outdoor environments, this study considered seven thermal comfort indices to identify the climatic impacts on human thermal comfort and quantify stress and discomfort levels. Namely, the predicted mean vote (PMV) discomfort Index (DI), cooling power index (CPI), Humidex, WBGT, SET and UTCI.

Predicted mean vote (PMV) index: Proposed by Fagner in 1970 to predict the thermal sensation vote (TSV) [40]. It predicts the mean response of a large group of people by a value according to the 7-step ASHRAE comfort scale [41]. The index is one of the most popular indices in human biometeorology [42]. It is described by the thermal load on the body, air temperature, mean radiant temperature, air speed, humidity, metabolic rate, and the insulation of the clothing of the individual [29]. Previous publications indicated several ranges of PMV regarding acceptability of thermal comfort. Some considered that the environment is thermally accepted when PMV range from -0.5 to 0.5 [43–46] and -0.85 to 0.85 [47], while others extended the range to -1 to 1 [48].

Discomfort index (DI): Proposed by Thom (1959) and was applied for quantifying the effective temperature [23,24]. It is also called the temperature-humidity index (THI) [49]. The discomfort index (DI) depends on two components, namely dry bulb temperature and relative humidity, which simplifies its evaluation [50].

Cooling power index (CPI): Introduced by Landsberrg for defining human comfort using the dry bulb temperature and wind speed [51]. Later, it was reported that the wind speed effect is minimal [52].

Humidex index: It was first used by Canadian meteorologists [53]. It describes thermal sensation in humid [54] or hot and humid climates [55], as it is considered to be a thermo-hygrometric index [56]. In comparison to (DI). Humidex is more sensitive to inputs' variation and change rate. It combines temperature and relative humidity and is always higher than ambient temperature.

Wet bulb globe temperature (WBGT) index: Recommended for examining heat stress incidents by the American army [57] and for human heat load estimations during large athletic events, such as Brazil world cup 2014 [58]. Ambient conditions, clothing insulation, human activities are taken into consideration [59]. The WBGT is a function of the wet bulb temperature, the globe temperature, and the dry bulb temperature. For shaded areas, the globe temperature is estimated to be equal to the dry bulb temperature.

Standard effective temperature (SET) index: Proposed by ASHRAE, the index is used for assessment of thermal comfort for normal daily conditions. The index is defined as the dry bulb temperature of a hypothetical isothermal environment of 50% relative humidity in which a subject, while wearing clothing standardized for activity concerned, would have the same heat stress and thermo-regulatory strain as in the actual test environment [60]. Isothermal environment refers to the environment at sea level, in which the air temperature is equal to the mean radiant temperature, and the air velocity is zero. SET temperature is calculated at a steady state surface skin temperature and wittedness after 60 min of exposure to the environment [61].

Universal Thermal Climate Index (UTCI): Developed in the early 2000's by European scientists and experts from Australia, Canada, Israel and New Zealand, for modeling and characterization of human response related thermos-physiological processes. The index is suitable for assessing meteorological, bioclimatic and environmental warnings. The index is claimed to be able to describe thermal comfort in all climates, seasons, and time and spatial scales [62]. Evaluating the UTCI includes a detailed clothing model [63] and a human thermophysiological processes model [64]. The detailed process for calculation can be found in Refs. [65–67]. The UTCI can be used to assess the thermal comfort in both indoor and outdoor environments, and can be used in both hot and cold climates [68,69]. The RayMan model [70], takes into account air temperature, air humidity and air velocity [71] and calculates the radiation fluxes for determining the mean radiant temperature. Mean radiant temperature value (MRT) is vital for investigating the human energy balance model and for assessing the human thermal comfort. The model is affected by the atmospheric conditions such as cloud cover, linked turbidity (a factor that describes the haziness of the atmosphere), day of year, time and albedo and data such as height, gender, activity and clothing insulation [72]. Blazejczyk et al. (2012) [73] compared the UTCI model to several thermal indices. In correlation with the UTCI index, the authors found that the SET, the effective temperature (ET), and the physiological temperature (PT) indices were the highest.

This paper presents a comparative study of the suitability of using seven thermal comfort indices as tools to assess outdoor thermal comfort in hot and arid environments. The indices, namely PMV, discomfort Index (DI), cooling power index (CPI), Humidex, WBGT, SET and UTCI, were validated against the TSV obtained from a thermal survey. The results of an online survey of the thermal comfort are compared to the thermal indices obtained from CFD simulations based on local climatic data. Thermal comfort surveys were performed during the Qatar Emir Cup on May 2017.

1.3. Motivation and objectives

This study aims to aid scientists, designers, and engineers in selecting representative thermal indices suitable for assessment of outdoor thermal comfort in hot and arid environments. The results of thermal sensation vote (TSV) are used for assessing several thermal comfort indices. The study also aims to compare the results obtained from a thermal comfort survey to other numerically calculated thermal indices. The performance of each thermal index was measured by evaluating the agreement between the thermal index predicted value and the value obtained from the TSV survey.

This paper is structured as follows: section 2 discusses the methods and tools used for evaluating the different thermal comfort indices. In section 3, the results from the survey and CFD simulations are presented and compared. Finally, in section 4, conclusions are drawn, and recommendations are given.

2. Materials and methods

In this section, the methodology used for conducting the survey and the numerical simulation setup is discussed. The section begins by detailing Khalifa international stadium's location and geometry, and then discussing the guidelines followed for constructing and performing the thermal comfort survey. Hence, the details for the CFD simulation setup are provided.

This paper aims to assess the use of different thermal comfort indices

in an air-conditioned stadium in hot and arid environment. The assessment is performed by comparing the results of a thermal comfort survey (TSV) to the thermal indices predicted by computational fluid dynamics (CFD) simulations. For validation, participants in the stadium were asked to fill in an online questionnaire about their thermal sensation. The thermal survey is conducted in an open air-conditioned stadium during a football game played in the evening. The responses of the questionnaire were used as a basis to assess the CFD predicted thermal comfort indices. Fig. 1 shows a flow diagram summarizing the methodology adopted in this paper for assessing the thermal comfort indices.

2.1. Khalifa international stadium geometric configuration

The thermal survey study was conducted during the Emir cup finals played at Khalifa international stadium, Doha, Qatar, 25°15′49.2″N 51°26′52.7″E. The stadium opened its doors in 1976 and has been expanded before the Asian games in 2006 to double its capacity to 40,000 spectators. The stadium is oriented North-South as specified by FIFA football stadiums handbook [74]. For performing CFD simulations, a three-dimensional model was built to simulate the stadium and its surroundings. As shown in Fig. 2, the stadium has main dimensions of $L \times W \times H = 290 \times 275 \times 69$ m.

2.2. Thermal comfort questionnaire

A total of 532 individuals participated on an online thermal survey during the Emir's Cup on the May 19, 2017 at Khalifa Stadium, in Doha, Qatar. The number of participants and their physical distribution within the stadium zones satisfied the standard of thermal comfort survey [26,75]. The area of individual stadium zones ranged between 30 m^2-60 m^2, requiring only three surveyed locations for each individual zone. The construction of the questionnaire followed the guidelines proposed by Cena and de Dear (2001); Hwang et al. (2006); Lai et al. (2014) [76–78].

The stadium was divided into six zones according to the tiers and the respondents had to identify their zone to complete the online survey. Fig. 3 shows the locations of the six zones and the distribution of participants at each zone. It also shows the number of the participating gender. The thermal survey included two main parts, the participant's background and their assessment of the thermal environment. The individual's background recorded the participant age, gender, and physical/medical conditions. As proposed by ASHRAE, the participants were asked to state their thermal sensation, using a 7-scale thermal sensation vote (TSV) [79,80]. Table 1 shows the TSV scale used in the survey to evaluate the participants' thermal comfort [81].

The online questionnaire included 13 questions. Participants were asked to declare their seating location and zone (Question No 1), to state their age and gender (Questions No 2 and 3), to report any medical issues (Question No 4), to describe their clothes (Questions No 5 to 7) and finally to assess their thermal comfort perception and to include comments (Questions No 8 to 13). The survey was completed after 2 h of the participants admittance to the stadium, so participants were fully acclimatized to the stadium's environment. Men comprised most of the audience with 466 respondents while women were less than 13%. Twenty of the participants (3.75%), three women and seventeen men, stated minor health issues (for example asthma or common cold). The questionnaire surveyed the individual's clothing style for assessment of the material insulation and selection of appropriate average clo values required for the indices' calculation. According to Köppen-Geiger climate classification, the Qatari climate is classified as hot desert climate (BWh). The letter 'B' refers to arid, 'W' refers to desert, and 'h' means 'hot' [82]. The Qatari climate is considered as arid [8] with temperature exceeding 40 °C [83–85]. Most of the male participants reported wearing *Thobs* and sandals or flip flops. Whereas the female participants indicated wearing *Abayas*. Thobs are considered to present a clothing insulation of 1.05–1.23 clo value while *Abayas* represent 1.19–1.24 clo value [86]. Arabian clothes proved to insulate adequately in hot and arid environments offering high levels of thermal comfort [87,88]. The participant demographic data is depicted in Fig. 4. For both genders, the dominant age group of the participants was 26–35 years, followed by the age group 18–25 years.

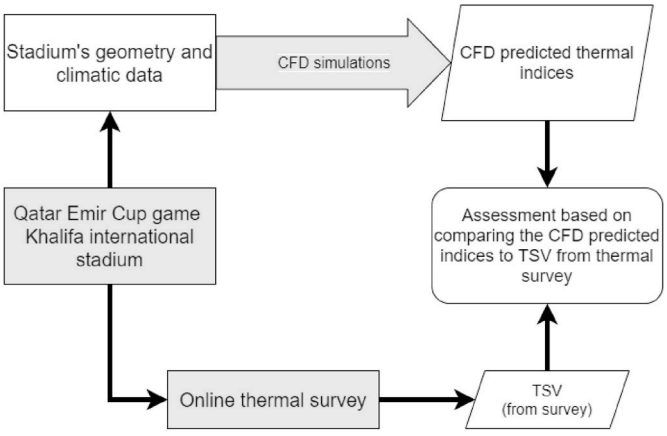

Fig. 1. Flow diagram for thermal indices assessment methodology.

2.3. Methodology for numerical simulations

2.3.1. Mathematical model

The numerical simulations were performing using the commercial CFD code ANSYS Fluent version 18.0. The CFD results were used to examine the flow field and the distribution of temperature and relative humidity within the stadium, which were used to obtain the thermal comfort indices. CFD simulations guidelines for urban environments provided by Blocken (2015) [89] were followed.

The CFD simulations utilized a pressure-based solver to solve the incompressible Navier-Stokes equations. The resulting pressure and velocity fields were used to solve the energy equation. The continuity and momentum equations that govern the steady fluid flow are considered as follows:

$$\nabla \cdot \mathbf{u} = 0, \tag{1a}$$

$$\mathbf{u} \cdot \nabla \mathbf{u} = \nu \nabla^2 \mathbf{u} - \frac{1}{\rho} \nabla p, \tag{1b}$$

where $\boldsymbol{u}$ is the velocity vector, ν is the kinematic viscosity of air, ρ is the air density, and p is the pressure. The energy equation and species transport models were considered to reflect the actual heat transfer and relative humidity levels, respectively. The steady state energy equation for an incompressible flow is given by:

$$\mathbf{u} \cdot \nabla T = \kappa \nabla^2 T - Q, \tag{2}$$

where T is the temperature of the fluid, κ is the fluid thermal conductivity, and Q is the volumetric heat flux. For a steady state flow without chemical reactions, the equation for species transport is considered as follows:

$$\mathbf{u} \cdot \nabla \varphi = -\nabla \cdot \mathbf{J} \tag{3}$$

where φ is the concentration of the species and $\mathbf{J}$ is the diffusion flux due to the gradient of species concentration. In this paper, a single species transport equation is solved for the water vapor concentration.

For turbulence modeling, the Reynolds-Averaged Navier Stokes (RANS) standard k- ε model was used. The model was developed in 1974, and presented a good compromise between prediction of turbulent quantities and computational efficiency [90]. Previous studies examined the suitability of the standard k- ε model for natural ventilation simulation [91–94].

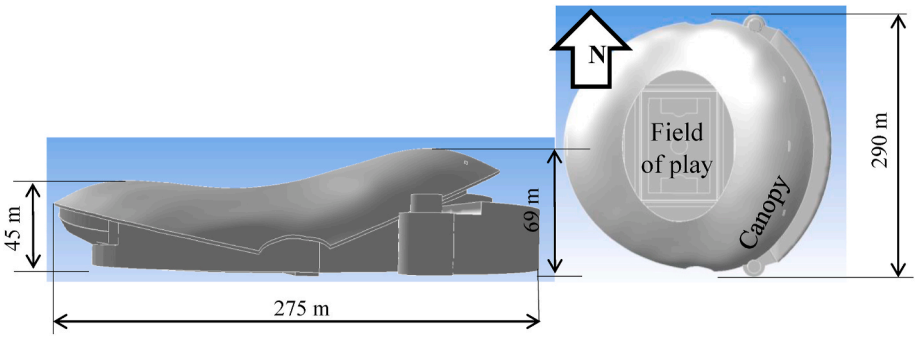

Fig. 2. Geometry of Khalifa international stadium.

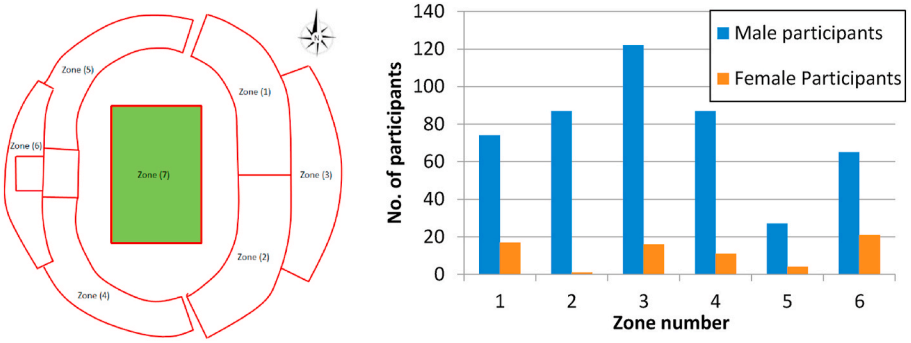

Fig. 3. Seating zones in the stadium and the distribution of participants per zone.

Table 1
Scales for thermal comfort [81].

Questions	"I feel … ''	"Temperature''	"Climate … ''	"Overall Experience''	"Rate Climate … ''
Possible answers	Hot +3 Warm +2 Slightly warm +1 Neutral 0 Slightly cool -1 Cool -2 Cold -3	Cooler The same Warmer	Highly acceptable +1 Acceptable 0 Unacceptable 0 Highly unacceptable -1	Comfortable Slightly uncomfortable Uncomfortable Very uncomfortable	Very satisfied Satisfied Somewhat satisfied Neutral Somewhat unsatisfied Unsatisfied Very unsatisfied

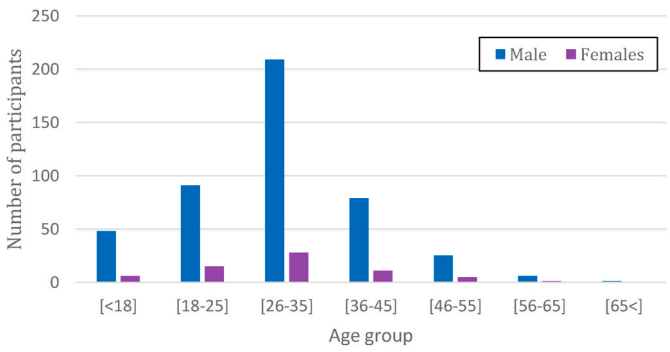

Fig. 4. Participants' demographic data.

The SIMPLE algorithm was used for the pressure-velocity coupling. The evaluation of the pressure gradients was performed by least-squares cell-based. The pressure discretization was of a second-order accuracy. A second-order upwind scheme was used to discretize the transport equations' convective terms.

2.3.2. Computational domain and grid

The stadium orientation, wind direction, computational domain and the surface mesh are shown in Fig. 5. The surface mesh depicting stadium's tiers, field of play and the refined grid near the air supply nozzles is illustrated in the figure. The computational domain dimensions were considered as $L \times W \times H = 2500 \times 2000 \times 300$ m^3 and a maximum blockage ratio of 2.5%, which was below the maximum good practice limit of 3% [71,72]. The distance from the building to the domain boundary was at least five times the height of the building. The distance from the building to the domain outlet was 15 times the height, as recommended by Franke (2007) and Tominaga et al. (2008) [95,96].

About 30 million hexahedral cells were used to discretize the computational domain for both the stadium and its surroundings. The grid size was selected according to a mesh independency study to ensure that the numerical solution results do not change with further mesh refinement. The computational domain grid size and quality parameters are detailed in Table 2.

2.3.3. Boundary conditions

For CFD simulations, the stadium outer walls were set to have zero heat flux. The field of play (FoP) conditioned air supply nozzles were simulated as velocity inlet boundary condition with 12 m/s air velocity and 10°C air temperature. While the spectators conditioned air supply nozzles were simulated as velocity inlet boundary condition with 2 m/s air velocity and 12°C air temperature and 55% relative humidity. During

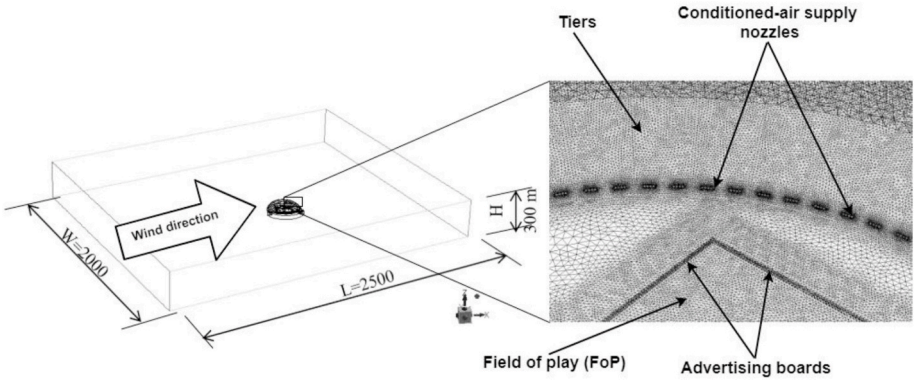

Fig. 5. Computational domain and surface mesh at the stadium's field of play and tiers.

Table 2
Grid size and quality parameters.

Grid size	Parameter	Value
	No. of cells	29630969
	No. of nodes	5288689
Quality parameters	Minimum orthogonal quality	0.014
	Maximum skewness	0.958
	Maximum aspect ratio	59.1

the game played on May 19, 2017, the measured ambient temperature was 36°*C*, and the relative humidity was 40%. The measured average wind speed was 2.2 m/s at a reference height of 10 m above the ground having a velocity profile changing with height according to equation (4). On that day, the prevailing direction of the blowing wind was NNW.

$$\frac{u}{u_r} = \left(\frac{y}{y_r}\right)^{\alpha} \tag{4}$$

where, u is the wind speed (m/s) at height y (m), and u_r is the known wind speed at a reference height y_r. The exponent α is an empirically derived coefficient that varies depending on the stability of the atmosphere. For this study, α was set to 0.143 to neglect the terrain outside the stadium.

Table 3 summarizes the boundary conditions used to simulate the stadium outer and inner environments. The model accounts for both sensible and latent heat generated by players, field of play (FoP), and the spectators in the stadium. Because the questionnaire was performed during night game, the radiation model was not used for the CFD simulations.

Table 3
Boundary conditions for numerical simulation.

Boundary Condition			Value	Units
Ambient	Inlet and outlet boundaries	Temperature	36	°C
		Relative humidity	40	%
		Prevailing wind	2.2	m/s
		Wind direction	NNW	
Tiers	Air supply	Temperature	12	°C
		Relative humidity	55	%
		Flowrate	25	l/s/person
		Velocity	2	m/s
	Sensible and latent heat generation	Sensible heat	90	W/person
		H_2O source	2.7227×10^{-5}	kg/m^{3}s
FoP	Air supply	Temperature	10	°C
		Velocity	12	m/s
	Sensible and latent heat generation	Energy source	37.15	W/m^3
		H_2O source	5.81×10^{-5}	kg/m^{3}s

For validation of the numerical simulation results, ambient air conditions inside and outside the stadium were simultaneously measured during the game played at night on the May 19, 2017. Air temperature, relative humidity, and wind velocity were measured at 58 locations within the stadium. Fig. 6 shows the locations of the 58 measuring points on the stadium's field of play (FoP), lower and upper tiers, and their corresponding zones.

The measurements were undertaken using multiple sets of Kestrel 5400 Heat stress tracker instrument. The device has the following specifications:

- Temperature measurements: accuracy of ±0.5 °*C*, resolution of 0.1°*C*
- Relative humidity: accuracy of ± 2% RH%, resolution of 0.1% RH
- Wind velocity: accuracy of 3%, resolution of 0.1 m/s

2.4. Evaluation of thermal comfort indices

In this subsection, the equations used for calculating the thermal comfort indices from the CFD simulation results are presented. For calculating the thermal comfort indices, an average clothing factor of 1.15 was used, and a metabolic rate M of 58 W/m^2 is selected to

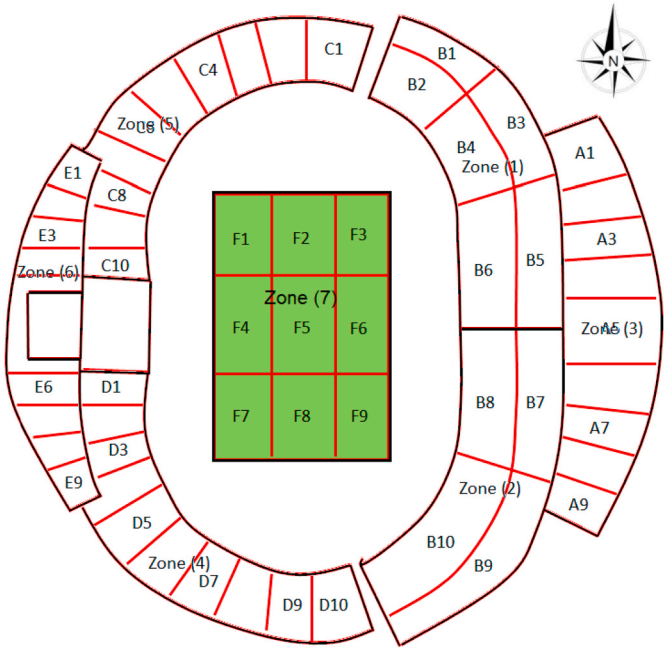

Fig. 6. Distribution of measuring locations over the stadium FoP and tiers.

represent a seated individual. The rate of mechanical work is taken to be equal to zero.

Predicted mean vote (PMV) index: The equation used for predicting the PMV value from the CFD results is as follows:

$$PMV = \left(0.303e^{-0.036M} + 0.028\right) \times L \quad (5)$$

where, M is the metabolic rate of human body (W/m^2), and L is the thermal load on the body (W/m^2). The thermal load L on the body was estimated by using a 4th order polynomial with the temperature. The mean comfort vote (MCV) is obtained by taking the average PMV values per stadium zone [97]. The PMV and MCV are compared to the TSV and mTSV values were obtained from the thermal comfort survey.

Discomfort index (DI): The discomfort index (DI) is evaluated as follows [23]:

$$DI = T_{db} - (0.55 - 0.005 \times RH\%) \times (T_{db} - 14.5) \quad (6)$$

where RH% is the relative humidity percentile (%), and T_{db} is the dry bulb temperature ($^{\circ}C$)

Cooling power index (CPI): The cooling power index can be calculated by using the following equation [98]:

$$CPI = \left(0.37 + 0.51 \times V^{0.63}\right) \times (36.5 - T_{db}) \quad (7)$$

where CPI is the cooling power index ($mcal/cm^2.s$), V is the air velocity (m/s) and T_{db} is the dry bulb temperature ($^{\circ}C$).

Humidex index: The humidex index is obtained as follows [54]:

$$H = T_{db} + \frac{5}{9} \times (P_v - 10) \quad (8a)$$

$$P_v = 6.112 \times \left(\frac{RH}{100}\right) \cdot \times 10e^{\left(\frac{7.5 \cdot T_{db}}{237.7 + T_{db}}\right)} \quad (8b)$$

where, H is Humidex, T_{db} is the dry bulb temperature ($^{\circ}C$), and e is the atmospheric pressure of water vapor (mm Hg).

Wet bulb globe temperature (WBGT) index: The WBGT formula includes the wet bulb temperature, the globe temperature and the dry bulb temperature as shown in equations (9a) and (9b).

$$WBGT = 0.7T_w + 0.2T_G + 0.1T \quad a(9a)$$

$$WBGT = 0.7T_w + 0.3T \quad G(9b)$$

Table 4
Thermal comfort indices in literature.

Index	Indoor/Outdoor	Equation	Range/Scale		References
Predicted mean vote (PMV)	Indoor and outdoor	$PMV = (0.303e^{-0.036M}) + 0.028) \times L$	-3	Cold	[29,41]
			-2	Cool	
			-1	Slightly cool	
			0	Neutral	
			1	Slightly warm	
			2	Warm	
			3	Hot	
Discomfort Index (°C)	Indoor and outdoor	$DI = T_{db} - (0.55 - 0.005 \times RH\%) \times (T_{db} - 14.5)$	˂21	No discomfort	[23,50,100, 101]
			21–24	Discomfort under 50% of the population	
			24–27	Discomfort over 50% of population	
			27–29	Most of population feels discomfort	
			29–32	Everyone feels stress	
			>32	State of medical emergency	
Cooling power index (mcal/cm²s)	Indoor and outdoor	$CPI = (0.37 + 0.51 \times V^{0.63}) \times (36.5 - T_{db})$	<5	Hot	[51,98]
			6–10	Mild	
			11–15	Cool	
			16–22	Cold	
			23–30	Very cold	
			>30	Extreme cold	
Humidex (°C)	Outdoor	$H = Tdb + \frac{5}{9} \times (P_v - 10)$	20–29	Comfortable	[102–105]
			30–39	Some discomfort	
			40–45	Great discomfort	
		$P_v = 6.112 \times \left(\frac{RH}{100}\right) \cdot \times 10e^{\left(\frac{7.5 \cdot T_{db}}{237.7 + T_{db}}\right)}$	45˂	Dangerous	
WBGT (°C)	Outdoor	$WBGT = 0.7T_w + 0.2T_G + 0.1T_a$	<24	No risk	[59,99, 106–111]
			24–29.3	Moderate	
			29.4–32.1	High	
		$WBGT = 0.7T_w + 0.3T_G$	≥32.2	Extreme	
SET (°C)	Indoor	$H_{sk} = h_s(t_{sk} - SET) + wh_{s,e}(p_{s,sk} - 0.5p_{SET})$	>37.5	Very hot (great discomfort)	[60,112–114]
			37.5–34.5	Hot (very unacceptable)	
			34.5–30	Warm uncomfortable/unacceptable	
			30–25.6	Slightly warm/unacceptable	
			25.6–22.2	Comfortable (acceptable)	
			22.5–17.5	Slightly cool/unacceptable	
			17.5–14.5	Cold (unacceptable)	
			14.5–10	Very unacceptable	
UTCI (°C)	Outdoor	6th order polynomial approximation [66]	>46	Extreme heat stress	[73,115]
			38–46	Very strong heat stress	
			32–38	Strong heat stress	
			26–32	Moderate heat stress	
			9–26	No thermal stress	
			0–9	Slight cold stress	
			-13–0	Moderated cold stress	
			-13-(-27)	Strong cold stress	
			-27-(-40)	Very strong cold stress	
			-40>	Extreme cold stress	

where, WBGT is the wet-bulb globe temperature (°C), T_w is the wet bulb temperature (°C), T_G is the black globe temperature (°C) and T_{db} is the dry bulb temperature (°C). For shaded areas, T_G was considered as the dry bulb temperature as shown in equation (9b) [99].

Standard effective temperature (SET) index: SET is described by the standard heat transfer and the evaporative heat transfer coefficients, the fraction of the wetted skin surface, the water vapor pressure at skin and the saturated water vapor pressure at SET [41]. The SET is calculated by simulating the thermophysiological behavior of the human body [26], as follows:

$$H_{sk} = h_s(t_{sk} - SET) + wh_{s,e}(p_{s,sk} - 0.5p_{SET}) \quad (10)$$

where, H_{sk} is the heat loss from skin (W/m^2), h_s is the standard heat transfer coefficient (W/m^2.°C), t_{sk} is the skin temperature (°C), w is the fraction of the wetted skin surface, $h_{s,e}$ is the standard evaporative heat transfer coefficient (W/m^{2}kPa), $p_{s,sk}$ is the water vapor pressure at skin, normally assumed to be that of saturated water vapor at t_{sk} (kPa), and p_{SET} is the saturated water vapor pressure at SET (kPa).

Universal Thermal Climate Index (UTCI): The UTCI was estimated using a 6th order polynomial approximation [66]. The detailed process for calculation can be found in Refs. [65–67].

Table 4 lists the thermal assessment indices considered in this study. Most of the thermal indices are intended to be used for the assessment of indoor environments. However, it is argued that the indoor thermal indices can be used for the thermal assessment of outdoor environments as well. Assuming that the outdoor environment is mechanically controlled to provide similar thermal comfort conditions to the indoor environment justifies using similar thermal comfort assessment indices [26].

3. Results and discussion

In this section, the results from the questionnaire and the CFD predicted thermal comfort indices are presented and discussed. The assessment of the performance of the different thermal comfort indices is performed by comparing the CFD predicted indices values to the TSV results obtained from the thermal comfort survey. Different thermal indices have different evaluation scales. For example, PMV is evaluated using a 7-scale criteria while the discomfort index is evaluated using a 6-scale criteria. Hence, a direct comparison between the indices cannot be performed. The obtained values of the TSV were used as the benchmark to establish a similar correlated range among indices.

3.1. Survey results

The measured environmental conditions of the stadium six zones are reported in Table 5. Zone1 was of the highest average temperature while zone 3 was of the highest average relative humidity. Fig. 7 depicts the distribution of the thermal sensation for each of the stadium's zones using the results from the survey. The figure also shows the distribution of thermal sensation for all zones.

Using the TSV from the questionnaire answers, the mean thermal sensation vote (mTSV) as described in equation (11), was calculated to define the human thermal sensation in each zone.

Table 5
Measured environmental conditions per zone.

Zone	Average temperature (°C)	Average relative humidity (%)	Average wind velocity (m/s)
1	24.8	38.7	0.45
2	24.6	39.5	0.7
3	24	44	0.7
4	22.8	43.8	0.7
5	21.5	42.5	0.85
6	23	42	0.8

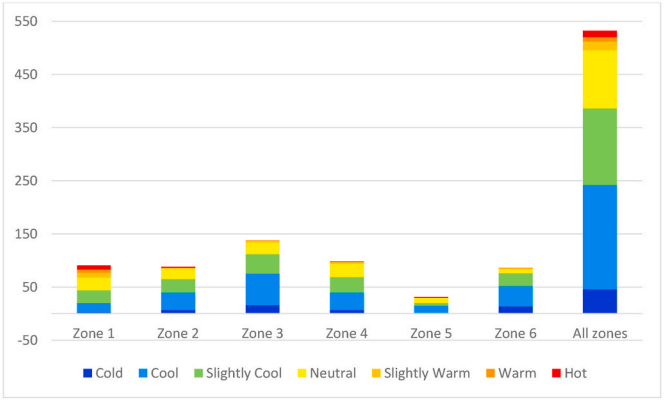

Fig. 7. Reported thermal sensation distribution per zone.

$$mTSV = \frac{Responses \times TSV}{Total\ Respondents} \quad (11)$$

Fig. 8 presents a box plot for the TSV values distribution at the stadium's zone. The box plot includes the average, minimum, maximum, and median values. The mTSV values for zones 2, 3, 4, 5 and zone 6 were within the thermally accepted range, indicating a "*Slightly Cool*" to "*Cool*" thermal sensation. Zone 6 proved to be the most thermally unaccepted (mTSV = -1.62) with Zone 3 to follow (mTSV = -1.43). During the event, Zone 1 (mTSV = -0.23) was found to be the highest thermally accepted zone in Khalifa stadium. Outdoor temperature is the main determinant for TSV affecting clothing and metabolic rate [116]. It is worth mentioning that zone 6 and zone 3 are located at the stadium highest tiers and are frequently exposed to infiltration of the outside hot wind through the roof oculus creating what is known as the ring of fire.

The thermal performance of zone 1, as the best thermally performed zone, and zone 6, as the worst thermally performed zone are further analyzed. Fig. 9 includes the answers for the two extreme zones. The scale used is known as the McIntyre scale, that indicates "*cooler*", "*the same*" and "*warmer*" answers as -1, 0, +1 respectively [117]. Although Zone 1 was the most thermally accepted location in the stadium, with mTSV ranging on the "cold'' side of the TSV scale, the total McIntyre scale value was (-0.44) indicating the individuals' expectations for even colder climate. Generally in hot climates, individuals prefer lower temperatures [117]. The overall thermal comfort of zone 6 was the lowest amongst the other zones. The individuals' expectation that the climate to become warmer as the McIntyre scale was (+0.19). Thus, the individuals taking part in this survey stated that in neutral conditions, they prefer colder environments.

Additionally, individuals who proposed the climate to remain "*the same*" stated a different thermal sensation other than neutral. Similar findings were recorded by Humphreys and Nicol (2004) [118]. For

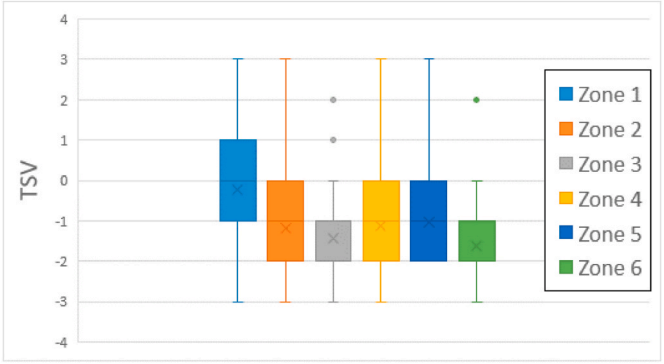

Fig. 8. Distribution of thermal sensation vote (TSV) values per zone.

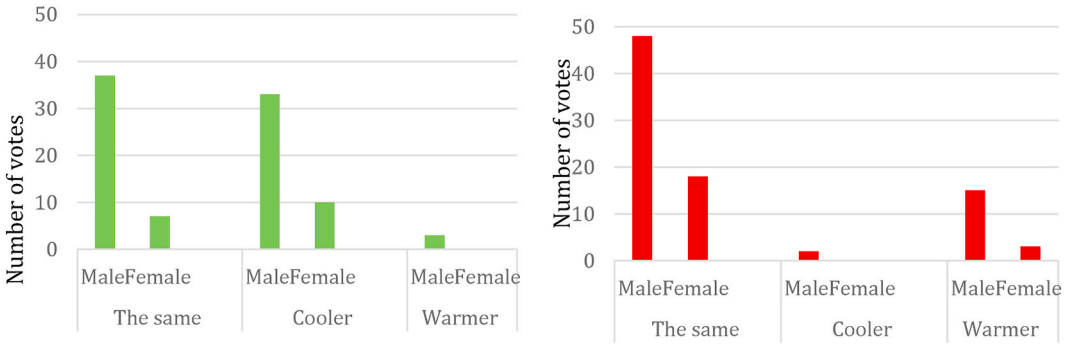

(a) zone 1 *(b) Zone 6*

Fig. 9. McIntyre scale votes for the preference for air temperature for (a) zone 1 and (b) zone 6.

"cold" thermal sensation, the individual's preference for higher temperature and warmer climates was recorded (as expected). The survey answers for the level of climate acceptability are depicted in Fig. 10.

Thermal acceptability is not distinctly nor clearly defined by ASHRAE Standard 55 and can be widely evaluated as an alternative for thermal comfort, referring to *"slightly cool"*, *"neutral"* and *"slightly warm"* thermal sensations [47]. Generally, some individuals can accept a specific climate although their thermal sensation vote might be off the (-1, 0, +1) range while others may state their thermal comfort as *"neutral* "without approving the climate acceptability [119]. Zone 1 presented the best mTSV values, close to *"neutral"* and as demonstrated by acceptability level, more than 90% of men (65 out of 72) and 88% of women (15 out of 17) favored the climate of zone 1. Similar behavior can be found for Zone 6, although it presented the lowest performance in terms of thermal comfort. More than 9 out of 10 men and women considered the climate to be *"acceptable"*.

3.2. CFD simulation results

3.2.1. Contour maps from CFD simulations

Figs. 11–13 show the contour maps of temperature, relative humidity and the air velocity obtained from CFD simulations. The results were plotted at a height of 0.5 m from the tiers surface and 1.5 m from the field of play. Fig. 11 depicts the contours of temperature for the stadium's tiers and field of play. A maximum temperature value of 21.7°C and an average temperature value of 20°C was captured on the FoP. A maximum temperature value of 26.2°C was depicted on the tiers near the stadium vomitories and on the upper tiers.

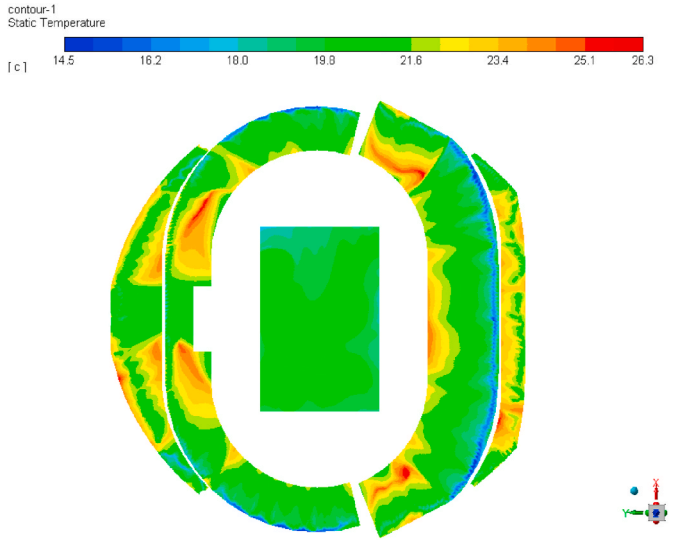

Fig. 11. Temperature contours at a plane 1.5 m high from the FoP and 0.5 m high from upper and lower tiers.

Figs. 12 and 13 shows the relative humidity and velocity contours. The relative humidity contours, Fig. 12, show a maximum relative humidity of 58.7% at the conditioned-air supply nozzles. Regions of minimum relative humidity of 34.7%, are coinciding with the areas of high

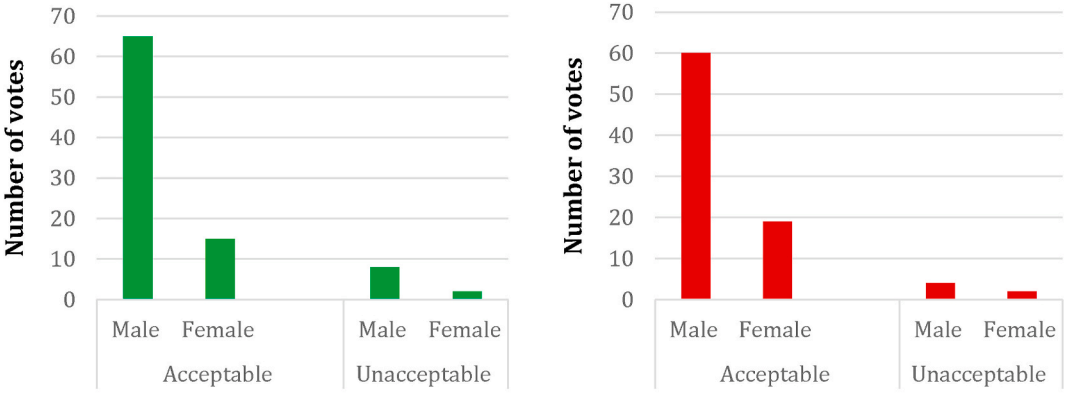

(a) Zone 1 *(b) Zone 2*

Fig. 10. Acceptability levels for (a) zone 1 and (b) zone 6.

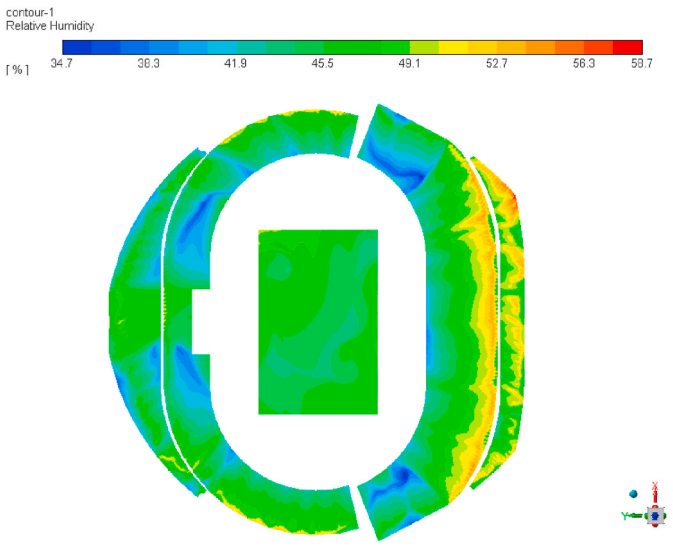

Fig. 12. Relative humidity contours at a plane 1.5 m high from the FoP and 0.5 m high from tiers.

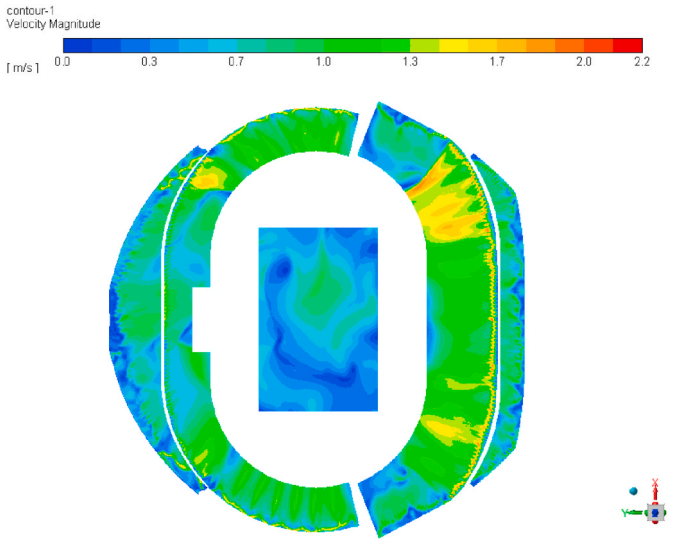

Fig. 13. Velocity contours at a plane 1.5 m high from the FoP and 0.5 m high from upper and lower tiers.

temperature values, as shown in Fig. 11. These relatively high temperature zones (hotspots) are attributed to the infiltration of outside hot air through the stadium open oculus and vomitories. The stadium average relative humidity value was 43.7%. As illustrated in in Fig. 13, the velocity contours have an average value of 0.73 m/s and a maximum velocity value of 2.2 m/s. Zones with high velocity values are those close to the air supply nozzles. In comparison to the stadium zones, the field of play velocity values were smaller, with an average value of 0.53 m/s.

3.2.2. *Validation of numerical simulation results*

The environmental measurements previously shown in Table 5 were used to validate the results from the numerical model. Figs. 14–16 show a comparison between measured and simulated values of temperature, relative humidity, and air velocity. In all figures, zone 7 refers to the stadium's field of play (FoP). As depicted in Fig. 14, the maximum temperature difference was in the order of 2°*C* for zone 4 with an average temperature difference of 1.3°*C* for all measured temperature values. The maximum relative humidity difference was 2% in zone 1 with an average difference of 0.5% (Fig. 15). Fig. 16 shows the

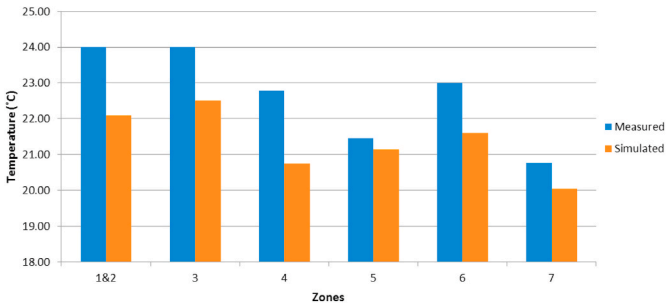

Fig. 14. Comparison between measured and simulated temperature in both tiers and FoP.

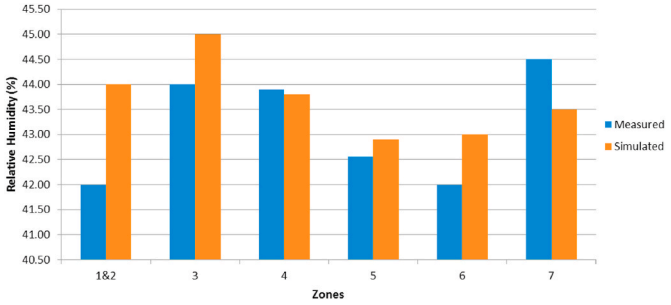

Fig. 15. Comparison between measured and simulated relative humidity in both tiers and FoP.

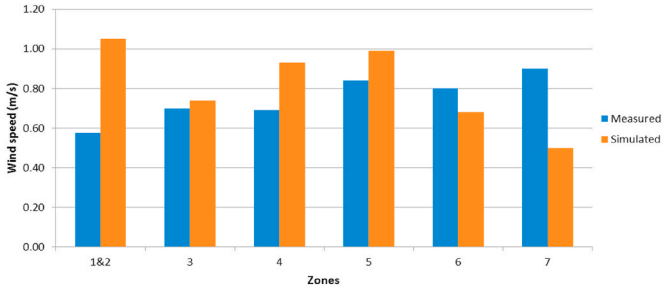

Fig. 16. Comparison between measured and simulated air speed in both tiers and FoP.

difference between measured and simulated wind velocity. The maximum difference was in the order of 0.48 m/s in zone 1 with an average difference of 0.06 m/s for all measured locations.

3.2.3. *CFD predicted thermal indices*

Figs. 17–23 show the contour maps of the seven thermal comfort indices as predicted from the CFD simulations. These results are used to obtain the average thermal comfort indices of the corresponding zones for comparison with the results obtained from the questionnaire.

3.2.3.1. PMV. As shown in Fig. 17, the average value of PMV index in a horizontal plane at height of 1.5 m from the field of play is -0.93 indicating a "*slightly cool*" thermal sensation. The contours shown for the tiers are plotted at a height of 0.5 m from the tiers' level, at a hight of the spectators' sitting positions. The maximum and minimum PMV values within the stadium were 0 and -2.5 respectively. These predicted values corresponded to as "*neutral*", "slightly cool", "*cool*" and "*cold*" thermal sensation (shaded range in Table 4). Lower values of PMV were generally recorded near the vicinity of the cold air supply nozzles.

3.2.3.2. Discomfort index. Predicted Discomfort index values are shown

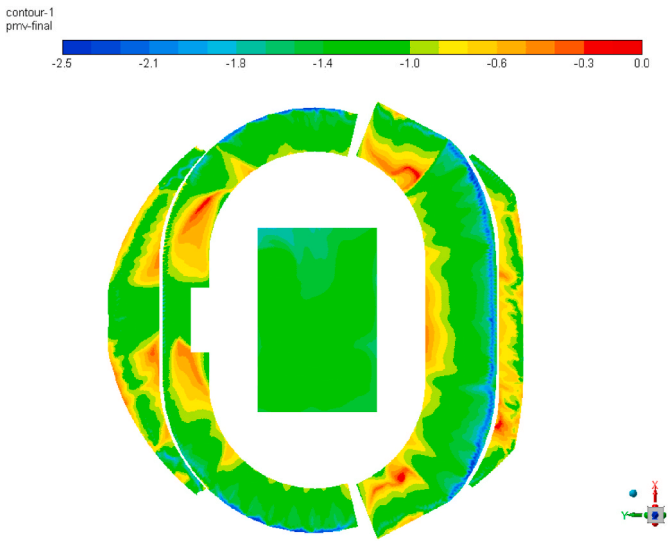

Fig. 17. PMV contours at a plane 1.5 m high from the FoP and 0.5 m high from tiers.

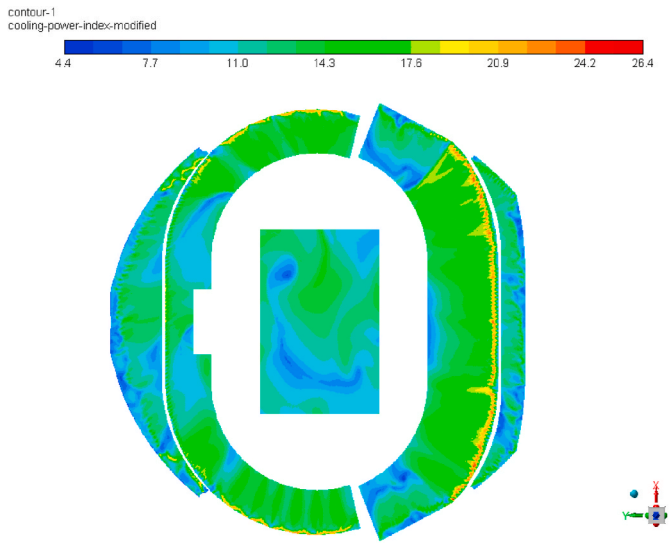

Fig. 19. Cooling power Index contours at a plane 1.5 m high from the FoP and 0.5 m high from tiers.

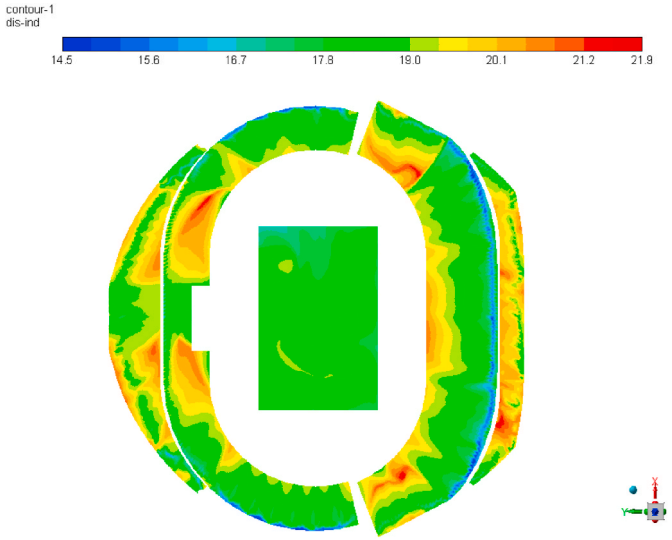

Fig. 18. Discomfort index (DI) contours at a plane 1.5 m high from the FoP and 0.5 m high from tiers.

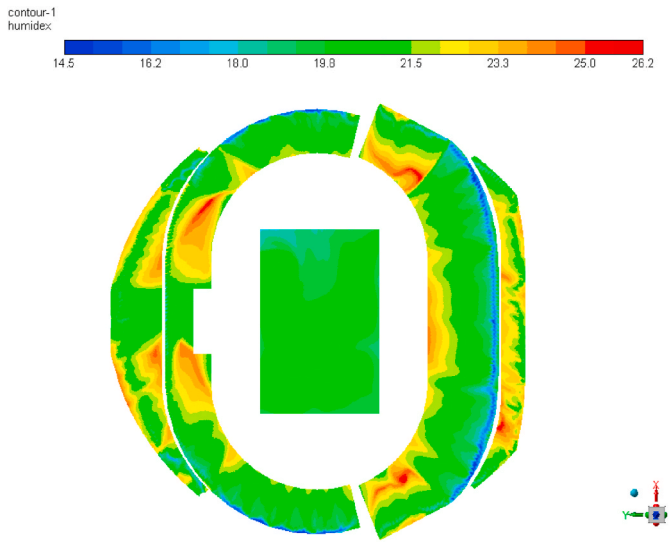

Fig. 20. Humidex contours at a plane 1.5 m high from the FoP and 0.5 m high from tiers.

in Fig. 18. The average simulated value of discomfort index in the field of play area was 18.3°*C*. While, for the spectators' area, the average predicted discomfort index was 19.2°*C*. Both values of the predicted discomfort index are lower than the 21°*C* threshold that indicates "*no discomfort*" on the discomfort index scale (shaded range in Table 4).

3.2.3.3. Cooling power index (CPI). The Cooling power index indicates the coldness of a zone. To calculate the cooling power index, Equation (7) was embedded in the CFD model as a user-defined function (UDF). Fig. 19 displays the cooling power index contours for the stadium field of play and tiers. A maximum cooling power index value of 24 mcal/cm^{2}s was recorded near the conditioned air supply nozzles. While, an average value of 12.5 mcal/cm^{2}s was recorded at an inclined plane passing through the spectators' head position at a height of 0.5 m. The value of 12.5 mcal/cm^{2}s corresponds to "*cool*" sensation on the cooling power index scale (shaded range in Table 4). Higher, colder, values of the cooling power index were generally recorded near the vicinity of the conditioned air supply nozzles.

3.2.3.4. Humidex. As depicted in Fig. 20, the stadium average predicted Humidex value was 21.6°*C* indicating a "*comfortable*" thermal sensation. Colder areas near the conditioned air supply nozzles were shown to have the minimum Humidex value of 20.15°*C* indicating a "*comfortable*" status as well. For the stadium occupied zones, the humidex index value was less than 27 corresponding to a "*comfortable*" sensation on the humidex scale (shaded range in Table 4).

3.2.3.5. WBGT. A User Defined Function (UDF) was embedded in the CFD model to calculate and display the WBGT contours. As shown in Fig. 21, the WBGT values ranged from a minimum of 16°*C* near the conditioned air supply nozzles to a maximum of 19°*C* near the stadium entrances and tiers vomitories. The average predicted value was 16.3°*C*. As these predicted values of WBGT is less than 24^{O}C, it indicates a "*no risk*" status on the WBGT scale (shaded range in Table 4).

3.2.3.6. SET. Fig. 22 shows the contours of the SET at the stadium's zones and field of play. A User Defined Function (UDF) was developed to

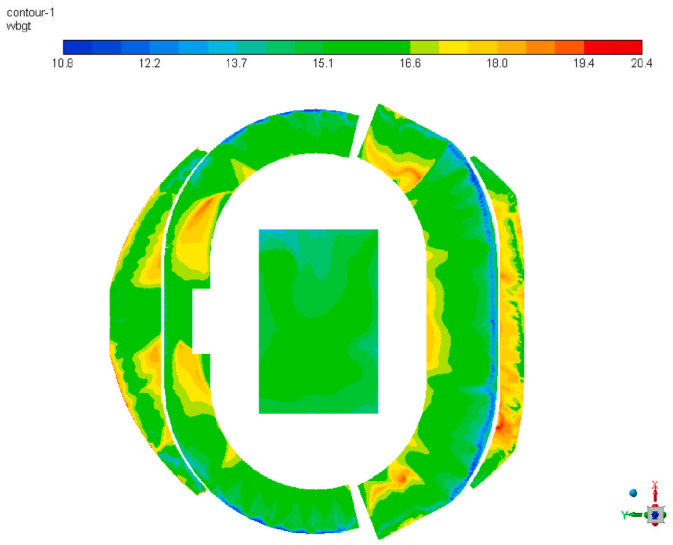

Fig. 21. WBGT contours at a plane 1.5 m high from the FoP and 0.5 m high from upper and lower tiers.

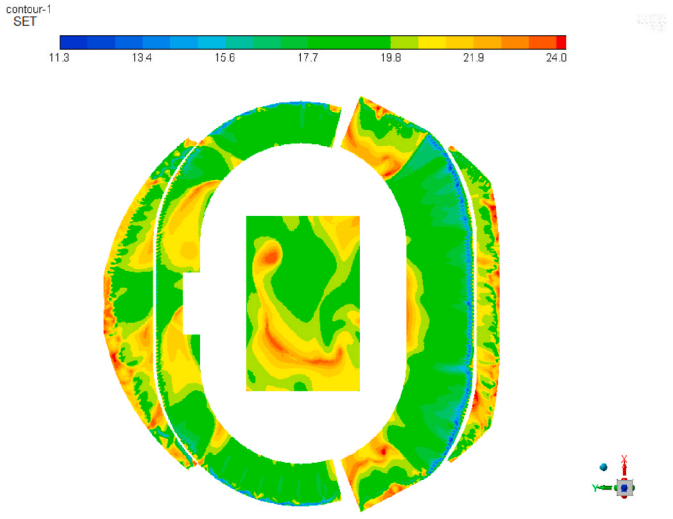

Fig. 22. SET contours at a plane 1.5 m high from the FoP and 0.5 m high from upper and lower tiers.

calculi the SET based on the ASHRAE Standard 55–2017 recommended method of calculation [26]. The SET values ranged from a minimum of 11.2°*C* to a maximum of 24°*C*. The average predicted SET value was 20.46°*C*. The SET values indicated "*comfortable*" and "*slightly cool*" thermal comfort levels on the SET scale (shaded range in Table 4).

3.2.3.7. UTCI. To calculate the UTCI values from the CFD simulations, a UDF was used. Fig. 23 shows the contours of the UTCI values at the stadium zones and field of play. The UTCI values ranged from a minimum of 8.4 °C near the conditioned air supply nozzles to a maximum of 25.5 °C near the stadium entrances and tiers vomitories. The UTCI average predicted value was 19.38 °C. The predicted UTCI values across the whole stadium indicate "*no thermal stress*" thermal conditions on the UTCI scale (shaded range in Table 4).

3.3. Comparison of predicted thermal comfort indices with questionnaire

The TSV data obtained from the questionnaire were compared to the CFD predicted values of seven thermal comfort indices. The TSV results

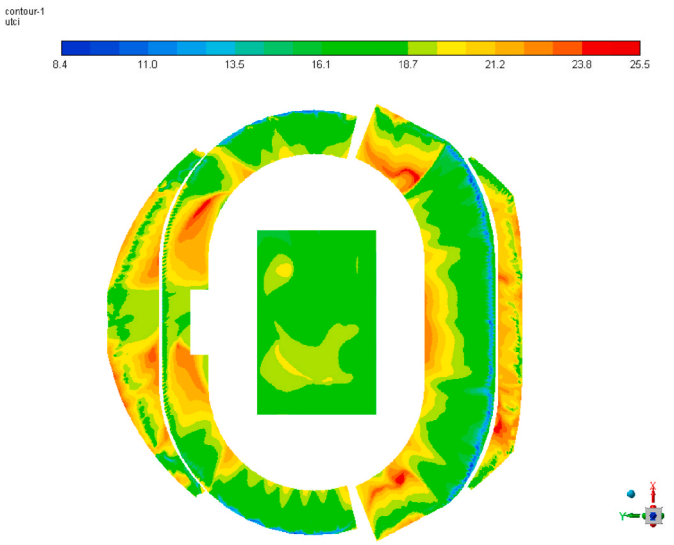

Fig. 23. UTCI contours at a plane 1.5 m high from the FoP and 0.5 m high from tiers.

from the questionnaire were used to obtain an equivalent thermal comfort index that can be directly compared to the CFD predicted values. The scales, shown in Table 4, were used to obtain an equivalent thermal index that corresponds to a certain TSV value. Figs. 24–30 compare the CFD predicted thermal indices to the survey results.

Fig. 24 depicts the differences between the questionnaire and predicted values of MCV for spectators. MCV values are obtained by averaging the PMV values previously shown in Fig. 17 and obtaining a single value for each zone. The maximum difference was recorded in zone 3 and it was around 0.9. Using Holmes method, the average error percentage of all zones was around 26% [120].

Fig. 25 depicts the differences between tiers real sensation and CFD predicted discomfort index (DI). Average values of DI were calculated for each zone. Maximum difference was noticed at zones 5 and zone 6, which was up to 4.5°*C*. The average error of all zones was around 15%.

The comparison between the questionnaire data and the predicted cooling power index (CPI) is depicted in Fig. 26. The index failed to estimate participants' real sensation. The average error of all zones was around 46%.

Fig. 27 compares the questionnaire and predicted values for the Humidex index. The maximum difference was recorded in zone 6 which was around 8.5 °*C*. Although the average error of all zones was around 16.5%, the model is still capable to estimate values close to the real sensation. The index main inherited disadvantage lies on the index-limited description of the environment to "*comfortable*" or "*some discomfort*" (*Table 4*).

Fig. 28 shows a comparison between the participants' real sensation

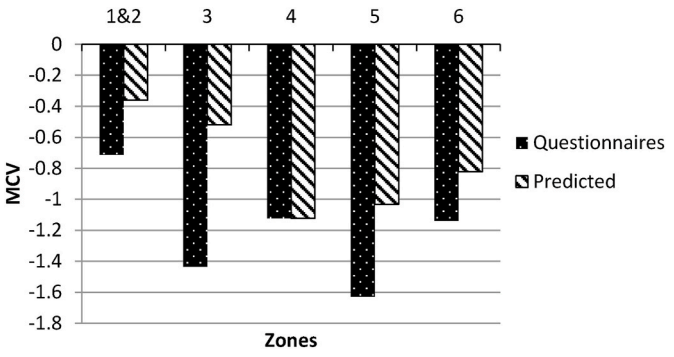

Fig. 24. Comparison between measured and predicted mean comfort vote.

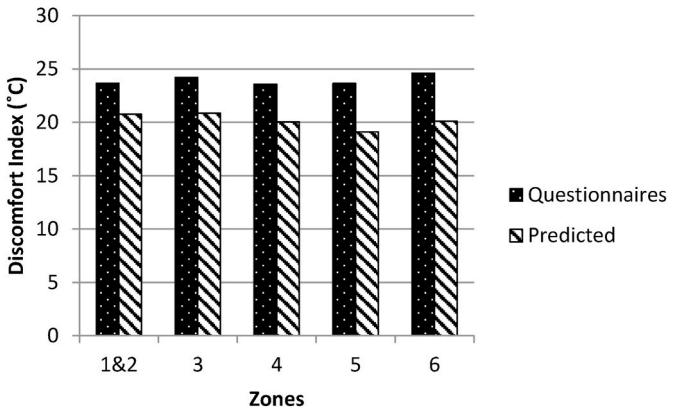

Fig. 25. Comparison between measured and predicted discomfort index (DI).

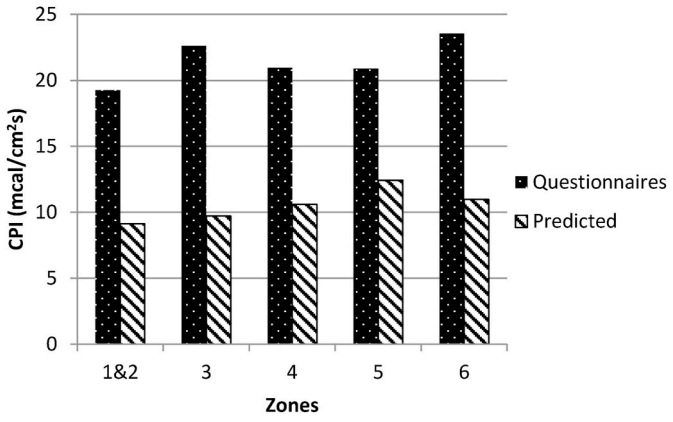

Fig. 26. Comparison between measured and predicted cooling power index (CPI).

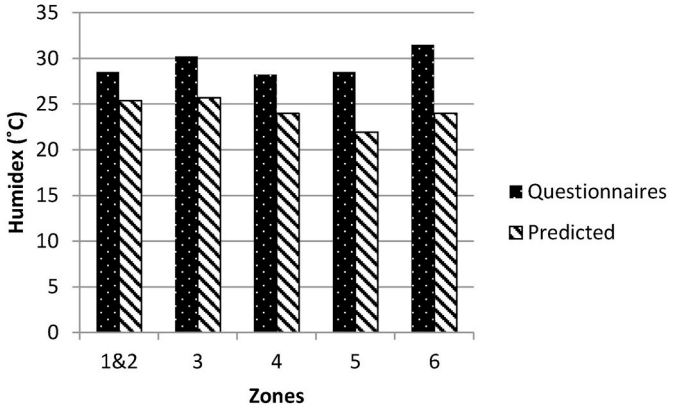

Fig. 27. Comparison between measured and predicted humidex.

and CFD predicted WBGT value for zones 1 to zone 6. A maximum difference of 3.3°*C* was depicted at zone 5. The average error for all the stadium zones was 8.8%. Comparison shows good agreement between both questionnaire and predicted data. The WBGT index is mainly used to assess the heat thermal risks in hot and arid environments. The index is not suitable to describe heat thermal risks in cold environments. Mainly, the index depends on site measured globe temperature. Although WBGT is able to predict a realistic thermal sensation, it is not always an available measure offered by the national weather stations.

CFD predicted standard effective temperature (SET) values were compared to questionnaire data for all the stadium zones. Fig. 29 shows

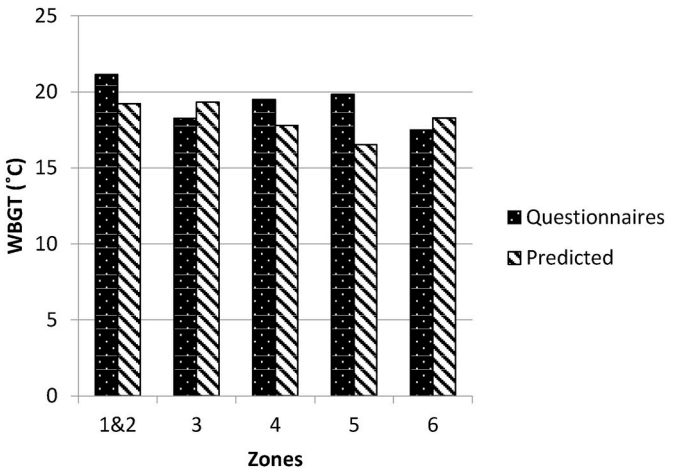

Fig. 28. Comparison between measured and predicted wet bulb globe temperature (WBGT).

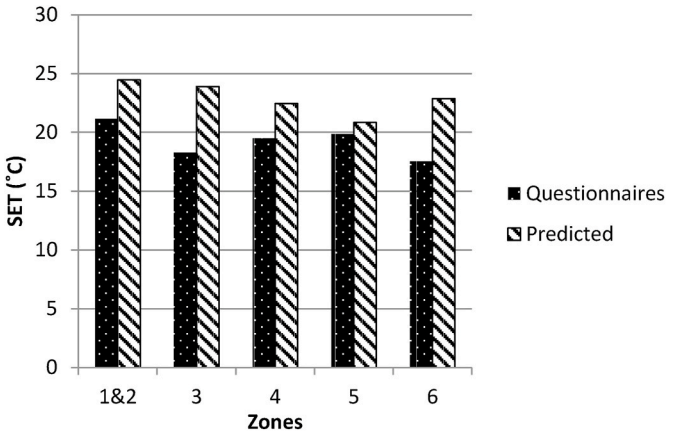

Fig. 29. Comparison between measured and predicted standard effective temperature (SET).

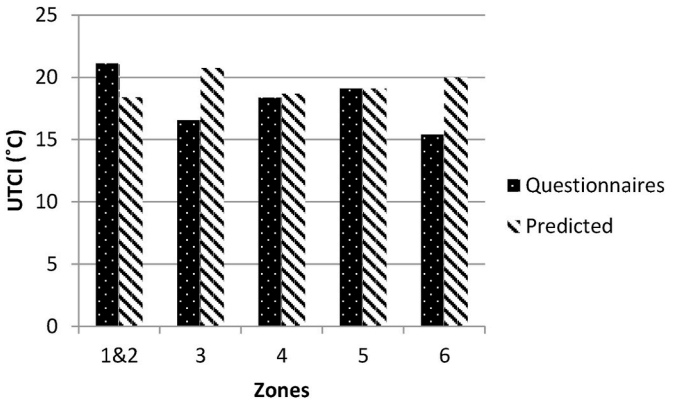

Fig. 30. Comparison between calculated and predicted UTCI.

the difference for all zones. A maximum difference of about 5.3°*C*. was noticed in zone 6. The average error of all zones was around 15%.

Fig. 30 shows the difference between the thermal survey results and the predicted CFD values of UTCI for spectator zones. The UTCI values were computed using a 6th order polynomial approximation [66]. The spectators thermal survey was carried in the hot environment of Doha, Qatar. Participants' thermal sensation responses reported as "*cool*" or "*cold*" were mapped as "*no thermal stress*" on the UTCI scale (Table 4).

Other participants thermal sensation responses reported as "*slightly warm*", "*warm*" and "*hot*" were considered as "*moderate heat stress*", "*strong heat stress*" and "*very strong heat stress*" on the UTCI scale (Table 4). A maximum difference between the calculated and the predicted UTCI values of about 29%. was recorded in zone 6. The average percentage difference of all zones was about 14%.

Fig. 31 summarizes the average error between CFD predicted thermal comfort indices and the real sensation of spectators obtained from the thermal comfort survey. The figure shows that the CFD prediction of WBGT value is the nearest to PMV values with an average difference of 8.8%, followed by the CFD prediction of UTCI model with an average difference of 14%. The performance of the UTCI CFD prediction model and the SET CFD prediction model was fairly similar within 15% difference to PMV values, which is consistent with the findings of previous literature [73]. The performance of the CPI CFD prediction model did not yield an accurate estimation of the thermal comfort level of the spectators.

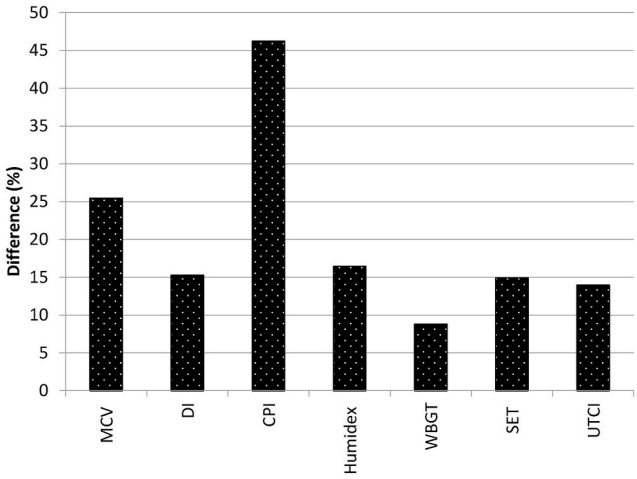

Fig. 31. Difference in percentage for the different thermal comfort indices.

4. Conclusions

This paper assessed the performance of seven thermal comfort indices using an online thermal survey and CFD predicted indices. An online thermal sensation survey was conducted on the May 19, 2017 for spectators attending the local Emir Cup in an air-conditioned stadium. The questionnaire provided the thermal sensation vote (TSV) for the respondents, which was used as a basis to assess the thermal comfort indices and the validate the CFD predicted indices.

The stadium was divided into six zones and a total of 532 individuals participated in the survey, recording their demographic data and indicating their personal thermal comfort perception. The majority of the respondents evaluated their thermal sensation as "*cool*" indicating high level of climate acceptability, although in literature "*cool*" sensation is out of range of the thermal acceptability description. The survey also indicated that individuals who stated a thermally "*neutral*" sensation would prefer the environment to become colder which agreed with previous research [7]. It could be concluded that humans from hotter demographic background prefer colder environments [121,122]. The results of the survey indicated high levels of climate acceptability, with small variations among the stadium zones and between genders.

CFD predicted MCV did not show good agreement with the thermal questionnaire with an average difference of 26%. For the DI, a maximum difference of $4.5^{\circ}C$ was noticed at zones 5 and 6. In comparison to the questionnaire, the average difference was 15%. The CFD model predicted SET and UTCI values within an average difference of about 15% to the surveyed to PMV values.

The value of the WBGT obtained by the CFD simulation showed the nearest results to the actual questionnaire data with an average difference of 8.8% which is consistent with previous related research work [5]. However, the WBGT index is mainly used to assess the heat thermal risk in hot environments. It depends on site measured globe temperature. The WBGT index is not suitable to assess heat thermal risk in cold environments. The CFD WBGT index model was able to predict a realistic thermal sensation. Nevertheless, the WBGT index typically is not recorded by national weather stations.

Humidex thermal comfort CFD model predicted the thermal comfort of the spectators with an average difference of 16.5%, but its main inherited disadvantage lies on the index limited range of description of the thermal environment to "*comfortable*" or "*some discomfort*". Other models have average difference between 15 and 26%, while only the CPI has an unacceptable average difference around 46%. It is concluded that the CPI index is not best suited to assess outdoor thermal comfort for hot and arid regions.

The results of the CFD predicted UTCI were in less agreement with the values calculated based on the questionnaire, with an average difference of 14%. In comparison to the calculation of the WBGT index, the calculation of the UTCI index is complicated and has the limitation of being applicable to temperature values between 50 °C and -50 °C. For hot climates, using the WBGT index to assess thermal comfort is preferred as it provides more reliable results, and the index is easier to compute. The CPI index deemed not suitable to assess outdoor thermal comfort for hot and arid regions.

Author statement

Saud Ghani: Conceptualization, Methodology, Writing - Original Draft, Writing - Review & Editing, Supervision, Funding acquisition

Ahmed Osama Mahgoub: Investigation, Writing - Original Draft, Writing - Review & Editing, Visualization.

Foteini Bakochristou: Formal analysis, Data Curation, Writing - Original Draft, Visualization.

Esmail A. ElBialy: Conceptualization, Methodology, Validation, Formal analysis, Methodology, Investigation, Writing - Original Draft, Visualization.

Declaration of competing interest

The authors declare that they have no known competing financial interests or personal relationships that could have appeared to influence the work reported in this paper.

Acknowledgement

The work presented in this paper was supported by a grant from the Qatar National Research Fund under its National Priorities Research Program [Award number NPRP 6-461-2-188] and the Aspire Zone Foundation [External grant number QUEX-CENG-ASPIRE-11/12-7]. The contents of this work are solely the responsibility of the authors and do not necessarily represent the official views of the Qatar National Research Fund. Open Access funding provided by the Qatar National Library.

References

[1] C.A. Njoku, M.T. Daramola, Human outdoor thermal comfort assessment in a tropical region: a case study, Earth Syst. Environ. 3 (2019) 29–42, https://doi.org/10.1007/s41748-019-00090-4.

[2] Z. Fang, X. Feng, J. Liu, Z. Lin, C.M. Mak, J. Niu, K.T. Tse, X. Xu, Investigation into the differences among several outdoor thermal comfort indices against field survey in subtropics, Sustain. Cities Soc. 44 (2019) 676–690, https://doi.org/10.1016/j.scs.2018.10.022.

[3] J. Spagnolo, R. de Dear, A field study of thermal comfort in outdoor and semi-outdoor environments in subtropical Sydney Australia, Build. Environ. 38 (2003) 721–738, https://doi.org/10.1016/S0360-1323(02)00209-3.

[4] A. Ugursal, C. Culp, An empirical thermal comfort model for transient metabolic conditions, ASHRAE Trans. 118 (2012) 742–750.

[5] Z. Wang, G. Wang, L. Lian, A field study of the thermal environment in residential buildings in Harbin, ASHRAE Trans. 109 (2003) 350–355.
[6] A.H.A. Mahmoud, Analysis of the microclimatic and human comfort conditions in an urban park in hot and arid regions, Build. Environ. 46 (2011) 2641–2656, https://doi.org/10.1016/j.buildenv.2011.06.025.
[7] T. Honjo, Thermal comfort in outdoor environment, Glob. Environ. Res. ©2009 AIRIES. 13 (2009) 43–47.
[8] S. Ghani, E.M. Bialy, F. Bakochristou, S.M.A. Gamaledin, M.M. Rashwan, B. Hughes, Thermal comfort investigation of an outdoor air-conditioned area in a hot and arid environment, Sci. Technol. Built Environ. 23 (2017) 1113–1131, https://doi.org/10.1080/23744731.2016.1267490.
[9] J. Toftum, L. Rasmussen, J. Mackeprang, Discomfort Due to Skin Humidity with Different Fabric Textures and Materials, ASHRAE, 2000.
[10] A.O. Mahgoub, S. Ghani, M.M. Rashwan, S.M. Ismail, E.A. ElBialy, Simulation of spectators' aerodynamic drag using porous models approximation, Build. Environ. 184 (2020), 107248, https://doi.org/10.1016/j.buildenv.2020.107248.
[11] B. Givoni, M. Noguchi, H. Saaroni, O. Pochter, Y. Yaacov, N. Feller, S. Becker, Outdoor comfort research issues, Energy Build. 35 (2003) 77–86, https://doi.org/10.1016/S0378-7788(02)00082-8.
[12] D. Lai, W. Liu, T. Gan, K. Liu, Q. Chen, A review of mitigating strategies to improve the thermal environment and thermal comfort in urban outdoor spaces, Sci. Total Environ. 661 (2019) 337–353, https://doi.org/10.1016/j.scitotenv.2019.01.062.
[13] A. Ghaffarianhoseini, U. Berardi, A. Ghaffarianhoseini, K. Al-Obaidi, Analyzing the thermal comfort conditions of outdoor spaces in a university campus in Kuala Lumpur, Malaysia, Sci. Total Environ. 666 (2019) 1327–1345, https://doi.org/10.1016/j.scitotenv.2019.01.284.
[14] M. Xu, B. Hong, R. Jiang, L. An, T. Zhang, Outdoor thermal comfort of shaded spaces in an urban park in the cold region of China, Build. Environ. 155 (2019) 408–420, https://doi.org/10.1016/j.buildenv.2019.03.049.
[15] K. Fabbri, A. Ugolini, A. Iacovella, A.P. Bianchi, The effect of vegetation in outdoor thermal comfort in archaeological area in urban context, Build. Environ. 175 (2020), 106816, https://doi.org/10.1016/j.buildenv.2020.106816.
[16] O. Potchter, P. Cohen, T.P. Lin, A. Matzarakis, Outdoor human thermal perception in various climates: a comprehensive review of approaches, methods and quantification, Sci. Total Environ. 631–632 (2018) 390–406, https://doi.org/10.1016/j.scitotenv.2018.02.276.
[17] X. Zhou, Q. Ouyang, Y. Zhu, C. Feng, X. Zhang, Experimental study of the influence of anticipated control on human thermal sensation and thermal comfort, Indoor Air 24 (2014) 171–177, https://doi.org/10.1111/ina.12067.
[18] Y. Wang, Z. Ni, Y. Peng, B. Xia, Local variation of outdoor thermal comfort in different urban green spaces in Guangzhou, a subtropical city in South China, Urban For. Urban Green. 32 (2018) 99–112, https://doi.org/10.1016/j.ufug.2018.04.005.
[19] J. Bouyer, J. Vinet, P. Delpech, S. Carré, Thermal comfort assessment in semi-outdoor environments: application to comfort study in stadia, J. Wind Eng. Ind. Aerod. 95 (2007) 963–976, https://doi.org/10.1016/j.jweia.2007.01.022.
[20] A.O. Mahgoub, S. Gowid, S. Ghani, Global evaluation of WBGT and SET indices for outdoor environments using thermal imaging and artificial neural networks, Sustain. Cities Soc. 60 (2020), 102182, https://doi.org/10.1016/j.scs.2020.102182.
[21] FIFA, Football Emergency Medicine Manual, Fédération Internationale de Football Association, Zurich, 2018.
[22] J.K. Vanos, E. Kosaka, A. Iida, M. Yokohari, A. Middel, I. Scott-Fleming, R. D. Brown, Planning for spectator thermal comfort and health in the face of extreme heat: the Tokyo 2020 Olympic marathons, Sci. Total Environ. 657 (2019) 904–917, https://doi.org/10.1016/j.scitotenv.2018.11.447.
[23] E.C. Thom, The discomfort index, Weatherwise 12 (1959) 57–61, https://doi.org/10.1080/00431672.1959.9926960.
[24] I. Kandjov, J. Ivancheva, A. Tzenkova, J. Ivancheva, Some biometeorological aspects of urban climate in Sofia, Proc. Fifth Int. Conf. Urban Clim. Lodz, Pol. 2 (2003) 103–106.
[25] T. Stathopoulos, H. Wu, J. Zacharias, Outdoor human comfort in an urban climate, Build. Environ. 39 (2004) 297–305, https://doi.org/10.1016/j.buildenv.2003.09.001.
[26] ANSI ASHRAE, ANSI ASHRAE Standard 55-2017: Thermal Environmental Conditions for Human Occupancy, 2017.
[27] ASHRAE, ASHRAE Handbook: Fundamentals I-P and SI Editions, ASHRAE, 2017.
[28] T.P. Lin, R. De Dear, R.L. Hwang, Effect of thermal adaptation on seasonal outdoor thermal comfort, Int. J. Climatol. 31 (2011) 302–312, https://doi.org/10.1002/joc.2120.
[29] M.A. Humphreys, J. Fergus Nicol, The validity of ISO-PMV for predicting comfort votes in every-day thermal environments, Energy Build. 34 (2002) 667–684, https://doi.org/10.1016/S0378-7788(02)00018-X.
[30] C.S. Fong, N. Aghamohammadi, L. Ramakreshnan, N.M. Sulaiman, P. Mohammadi, Holistic recommendations for future outdoor thermal comfort assessment in tropical Southeast Asia: a critical appraisal, Sustain. Cities Soc. 46 (2019), 101428, https://doi.org/10.1016/j.scs.2019.101428.
[31] J.Y. Deng, N.H. Wong, Impact of urban canyon geometries on outdoor thermal comfort in central business districts, Sustain. Cities Soc. 53 (2020), 101966, https://doi.org/10.1016/j.scs.2019.101966.
[32] U. Berardi, J. Graham, Investigation of the impacts of microclimate on PV energy efficiency and outdoor thermal comfort, Sustain. Cities Soc. 62 (2020), 102402, https://doi.org/10.1016/j.scs.2020.102402.
[33] I.A. Balogun, M.T. Daramola, The outdoor thermal comfort assessment of different urban configurations within Akure City, Nigeria, Urban Clim. 29 (2019), 100489, https://doi.org/10.1016/j.uclim.2019.100489.
[34] F. Binarti, M.D. Koerniawan, S. Triyadi, S.S. Utami, A. Matzarakis, A review of outdoor thermal comfort indices and neutral ranges for hot-humid regions, Urban Clim. 31 (2020) 100531, https://doi.org/10.1016/j.uclim.2019.100531.
[35] M.H. Elnabawi, N. Hamza, Behavioural perspectives of outdoor thermal comfort in urban areas: a critical review, Atmosphere (Basel) 11 (2019) 51, https://doi.org/10.3390/atmos11010051.
[36] P.K. Cheung, C.Y. Jim, Improved assessment of outdoor thermal comfort: 1-hour acceptable temperature range, Build. Environ. 151 (2019) 303–317, https://doi.org/10.1016/j.buildenv.2019.01.057.
[37] M.E. Matallah, D. Alkama, A. Ahriz, S. Attia, Assessment of the outdoor thermal comfort in oases settlements, Atmosphere (Basel) 11 (2020), https://doi.org/10.3390/atmos11020185.
[38] N. Nazarian, J.A. Acero, L. Norford, Outdoor thermal comfort autonomy: performance metrics for climate-conscious urban design, Build. Environ. 155 (2019) 145–160, https://doi.org/10.1016/j.buildenv.2019.03.028.
[39] T. Sharmin, K. Steemers, M. Humphreys, Outdoor thermal comfort and summer PET range: a field study in tropical city Dhaka, Energy Build. 198 (2019) 149–159, https://doi.org/10.1016/j.enbuild.2019.05.064.
[40] J. Liang, R. Du, Thermal comfort control based on neural network for HVAC application, in: Proc. 2005 IEEE Conf. Control Appl., IEEE, Toronto, Canada, 2005, pp. 819–824, https://doi.org/10.1109/cca.2005.1507230.
[41] G. Ye, C. Yang, Y. Chen, Y. Li, A new approach for measuring predicted mean vote (PMV) and standard effective temperature (SET*), Build. Environ. 38 (2003) 33–44, https://doi.org/10.1016/S0360-1323(02)00027-6.
[42] H. Mayer, P. Höppe, Thermal comfort of man in different urban environments, Theor. Appl. Climatol. 38 (1987) 43–49, https://doi.org/10.1007/BF00866252.
[43] R. Kosonen, F. Tan, Assessment of productivity loss in air-conditioned buildings using PMV index, Energy Build. 36 (2004) 987–993, https://doi.org/10.1016/j.enbuild.2004.06.021.
[44] K. Yonezawa, Comfort air-conditioning control for building energy-saving, in: Ind. Electron. Soc. 2000. IECON 2000. 26th Annu. Conference IEEE, IEEE, 2000, pp. 1737–1742, https://doi.org/10.1109/IECON.2000.972538.
[45] A. Pourshaghaghy, M. Omidvari, Examination of thermal comfort in a hospital using PMV-PPD model, Appl. Ergon. 43 (2012) 1089–1095, https://doi.org/10.1016/j.apergo.2012.03.010.
[46] A. Mochida, H. Yoshino, T. Takeda, T. Kakegawa, S. Miyauchi, Methods for controlling airflow in and around a building under cross-ventilation to improve indoor thermal comfort, J. Wind Eng. Ind. Aerod. 93 (2005) 437–449, https://doi.org/10.1016/j.jweia.2005.02.003.
[47] R.J. de Dear, G.S. Brager, Thermal comfort in naturally ventilated buildings: revisions to ASHRAE Standard 55, Energy Build. 34 (2002) 549–561, https://doi.org/10.1016/S0378-7788(02)00005-1.
[48] S.P. Corgnati, M. Filippi, S. Viazzo, Perception of the thermal environment in high school and university classrooms: subjective preferences and thermal comfort, Build, Environ 42 (2007) 951–959, https://doi.org/10.1016/j.buildenv.2005.10.027.
[49] T. Dombo, Geospatial Modeling of Human Thermal Comfort in Akure Metropolis Using Thom ' S Discomfort Index, 2019.
[50] I. Tselepidaki, M. Santamouris, C. Moustris, G. Poulopoulou, Analysis of the summer discomfort index in Athens, Greece, for cooling purposes, Energy Build. 18 (1992) 51–56, https://doi.org/10.1016/0378-7788(92)90051-H.
[51] H.E. Landsberrg, The Assessment of Human Bioclimate, Geneva, Switzerland, 1972.
[52] R. Aynsley, M. Spruill, Thermal comfort models for outdoor thermal comfort in warm humid climates and probabilities of low wind speeds, J. Wind Eng. Ind. Aerod. 36 (1990) 481–488, https://doi.org/10.1016/0167-6105(90)90331-6.
[53] R.B. Crowe, Recreation, tourism and climate-A Canadian perspective, Weather 30 (1975) 248–254, https://doi.org/10.1002/j.1477-8696.1975.tb05308.x.
[54] R. Rana, B. Kusy, R. Jurdak, J. Wall, W. Hu, Feasibility analysis of using humidex as an indoor thermal comfort predictor, Energy Build. 64 (2013) 17–25, https://doi.org/10.1016/j.enbuild.2013.04.019.
[55] M. Lukić, M. Pecelj, B. Protić, D. vic Filipović, J. Geogr, Inst Jovan Cvijic, SASAZbornik, An evaluation of summer discomfort in Niš (Serbia) using Humidex. 69, Rad. Geogr. Inst. Jovan Cvijic, SANU. 69 (2) (2019) 109–122, https://doi.org/10.2298/ijgi1301011m, 109–122.
[56] I. Charalampopoulos, A comparative sensitivity analysis of human thermal comfort indices with generalized additive models, Theor. Appl. Climatol. (2019) 1605–1622, https://doi.org/10.1007/s00704-019-02900-1.
[57] C.P. Yaglou, D. Minaed, Control of heat casualties at military training centers, Arch.Industr. Health 16 (1957) 302–316, https://doi.org/10.1017/CBO9781107415324.004.
[58] G.P. Nassis, J. Brito, J. Dvorak, H. Chalabi, S. Racinais, The association of environmental heat stress with performance: analysis of the 2014 FIFA World Cup Brazil, Br. J. Sports Med. 49 (2015) 609–613, https://doi.org/10.1136/bjsports-2014-094449.
[59] G.M. Budd, Wet-bulb globe temperature (WBGT)-its history and its limitations, J. Sci. Med. Sport 11 (2008) 20–32, https://doi.org/10.1016/j.jsams.2007.07.003.
[60] A.P. Gagge, A.P. Fobelets, L.G. Berglund, A standard predictive index of human response to the thermal environment, ASHRAE Trans.; (United States). 92 (1986) 2B.
[61] M. Fountain, C. Huizenga, A thermal comfort prediction tool, ASHRAE J. 38 (1996), https://doi.org/10.1080/09613218.2011.556008.

[62] G. Jendritzky, R. de Dear, G. Havenith, UTCI-Why another thermal index? Int. J. Biometeorol. 56 (2012) 421–428, https://doi.org/10.1007/s00484-011-0513-7.

[63] G. Havenith, D. Fiala, K. Błazejczyk, M. Richards, P. Bröde, I. Holmér, H. Rintamaki, Y. Benshabat, G. Jendritzky, The UTCI-clothing model, Int. J. Biometeorol. 56 (2012) 461–470, https://doi.org/10.1007/s00484-011-0451-4.

[64] K. Katić, R. Li, W. Zeiler, Thermophysiological models and their applications: a review, Build. Environ. 106 (2016) 286–300, https://doi.org/10.1016/j.buildenv.2016.06.031.

[65] P. Bröde, G. Jendritzky, D. Fiala, G. Havenith, The universal thermal climate index UTCI in operational use, Proc. Conf. Adapt. Chang. New Think. Comf. Wind. (2010) 9–11, 2010.

[66] P. Bröde, D. Fiala, K. Blazejczyk, Calculating UTCI Equivalent Temperature, … XIII, Univ, 2009, pp. 1–5.

[67] M. Richards, G. Havenith, Progress towards the final UTCI model, in: Proc. 12ˆ{th} {I}nternational {C}onference {E}nvironment {E}rgonomics, 2007, pp. 521–524.

[68] F. Wu, X. Yang, Z. Shen, Regional and seasonal variations of outdoor thermal comfort in China from 1966 to 2016, Sci. Total Environ. 665 (2019) 1003–1016, https://doi.org/10.1016/j.scitotenv.2019.02.190.

[69] J. Du, C. Sun, Q. Xiao, X. Chen, J. Liu, Field assessment of winter outdoor 3-D radiant environment and its impact on thermal comfort in a severely cold region, Sci. Total Environ. 709 (2020), 136175, https://doi.org/10.1016/j.scitotenv.2019.136175.

[70] M.R.M. Daneshvar, A. Bagherzadeh, T. Tavousi, Assessment of bioclimatic comfort conditions based on physiologically equivalent temperature (PET) using the RayMan model in Iran, Cent. Eur. J. Geosci. 5 (2013) 53–60, https://doi.org/10.2478/s13533-012-0118-7.

[71] A. Matzarakis, F. Rutz, Application of the RayMan model in urban environments, in: Ninth Symp. Urban Environ., Meteorological Institute, University of Freiburg, 2010.

[72] I. Charalampopoulos, I. Tsiros, A. Chronopoulou-Sereli, A. Matzarakis, Analysis of thermal bioclimate in various urban configurations in Athens, Greece, Urban Ecosyst. 16 (2013) 217–233, https://doi.org/10.1007/s11252-012-0252-5.

[73] K. Blazejczyk, Y. Epstein, G. Jendritzky, H. Staiger, B. Tinz, Comparison of UTCI to selected thermal indices, Int. J. Biometeorol. 56 (2012) 515–535, https://doi.org/10.1007/s00484-011-0453-2.

[74] FIFA, in: Football Stadiums: Technical Recommendations and Requirements, fifth ed., Féderationé Internationalé de Football Association (FIFA), 2011.

[75] GB/T 33658-2017, - Thermal Comfort Requirements and Evaluation for Indoor Environment, MOHURD and AQSIQ China, Beijing, 2017.

[76] K. Cena, R. de Dear, Thermal comfort and behavioural strategies in office buildings located in a hot-arid climate, J. Therm. Biol. 26 (2001) 409–414, https://doi.org/10.1016/S0306-4565(01)00052-3.

[77] R.-L. Hwang, T.-P. Lin, N.-J. Kuo, Field experiments on thermal comfort in campus classrooms in Taiwan, Energy Build. 38 (2006) 53–62, https://doi.org/10.1016/j.enbuild.2005.05.001.

[78] D. Lai, D. Guo, Y. Hou, C. Lin, Q. Chen, Studies of outdoor thermal comfort in northern China, Build. Environ. 77 (2014) 110–118, https://doi.org/10.1016/j.buildenv.2014.03.026.

[79] G. Donnini, J. Molina, C. Martello, D. Ho Ching Lai, K. Ho Lai, C. Yu Chang, M. Laflamme, V. Hiep Nguyen, F. Haghighat, Field Study of Occupant Comfort and Office Thermal Environments in a Cold Climate, Atlanta, 1996.

[80] M.A. Humphreys, M. Hancock, Do people like to feel 'neutral'? Energy Build. 39 (2007) 867–874, https://doi.org/10.1016/j.enbuild.2007.02.014.

[81] E. Johansson, S. Thorsson, R. Emmanuel, E. Kr, ?ger, Instruments and methods in outdoor thermal comfort studies. The need for standardization, Urban Clim. 10 (2014) 346–366, https://doi.org/10.1016/j.uclim.2013.12.002.

[82] H.E. Beck, N.E. Zimmermann, T.R. McVicar, N. Vergopolan, A. Berg, E.F. Wood, Present and future köppen-geiger climate classification maps at 1-km resolution, Sci. Data. 5 (2018) 1–12, https://doi.org/10.1038/sdata.2018.214.

[83] S. Attia, Assessing the Thermal Performance of Bedouin Tents in Hot Climates, 2014.

[84] J.A. Bryant, S. Law, A. Amato, A. Al Abdulla, Integrated project and metering design for the first passivhaus in Qatar, ASHRAE Trans. 119 (2013) 1–8.

[85] S. Ghani, E.A. ElBialy, F. Bakochristou, S.M.A. Gamaledin, M.M. Rashwan, B. Hughes, Thermal performance of stadium's Field of Play in hot climates, Energy Build. 139 (2017) 702–718, https://doi.org/10.1016/j.enbuild.2017.01.059.

[86] ASHRAE55:2004, ANSI/ASHRAE 55:2004 thermal environmental conditions for human occupancy, Ashrae (2004) 30, https://doi.org/10.1007/s11926-011-0203-9, 2004.

[87] F.F. Al-ajmi, D.L. Loveday, K.H. Bedwell, G. Havenith, Thermal insulation and clothing area factors of typical Arabian Gulf clothing ensembles for males and females: measurements using thermal manikins, Appl. Ergon. 39 (2008) 407–414, https://doi.org/10.1016/j.apergo.2007.10.001.

[88] G. Havenith, K. Kuklane, J. Fan, S. Hodder, Y. Ouzzahra, K. Lundgren, Y. Au, D. Loveday, A database of dtatic clothing thermal insulation and vapor permeability values of non-western ensembles for use in ASHRAE standard 55, ISO 7730, and ISO 9920, in: ASHRAE Trans, ASHRAE, Chicago, IL, 2015.

[89] B. Blocken, Computational Fluid Dynamics for urban physics: importance, scales, possibilities, limitations and ten tips and tricks towards accurate and reliable simulations, Build. Environ. 91 (2015) 219–245, https://doi.org/10.1016/j.buildenv.2015.02.015.

[90] B.E. Launder, D.B. Spalding, The numerical computation of turbulent flows, Comput. Methods Appl. Mech. Eng. 3 (1974) 269–289, https://doi.org/10.1016/0045-7825(74)90029-2.

[91] P.F. Linden, The fluid mechanics of natural ventilation, Annu. Rev. Fluid Mech. 31 (1999) 201–238, https://doi.org/10.1146/annurev.fluid.31.1.201.

[92] G. Ziskind, V. Dubovsky, R. Letan, Ventilation by natural convection of a one-story building, Energy Build. 34 (2002) 91–101, https://doi.org/10.1016/S0378-7788(01)00080-9.

[93] U. Drori, G. Ziskind, Induced ventilation of a one-story real-size building, Energy Build. 36 (2004) 881–890, https://doi.org/10.1016/j.enbuild.2004.02.006.

[94] U. Drori, V. Dubovsky, G. Ziskind, Experimental verification of induced ventilation, J. Environ. Eng. 131 (2005) 820–826, https://doi.org/10.1061/(ASCE)0733-9372(2005)131:5(820).

[95] J. Franke, Best Practice Guideline for the CFD Simulation of Flows in the Urban Environment, Meteorol. Inst., 2007.

[96] Y. Tominaga, A. Mochida, R. Yoshie, H. Kataoka, T. Nozu, M. Yoshikawa, T. Shirasawa, AIJ guidelines for practical applications of CFD to pedestrian wind environment around buildings, J. Wind Eng. Ind. Aerod. 96 (2008) 1749–1761, https://doi.org/10.1016/j.jweia.2008.02.058.

[97] A.O. Adunola, Evaluation of urban residential thermal comfort in relation to indoor and outdoor air temperatures in Ibadan, Nigeria, Build. Environ. 75 (2014) 190–205, https://doi.org/10.1016/j.buildenv.2014.02.007.

[98] C. Balaras, I. Tselepidaki, M. Santamouris, D. Asimakopoulos, Calculations and statistical analysis of the environmental cooling power index for Athens, Greece, Energy Convers. Manag. 34 (1993) 139–146, https://doi.org/10.1016/0196-8904(93)90155-4.

[99] B. Lemke, T. Kjellstrom, Calculating workplace WBGT from meteorological data: a tool for climate change assessment, Ind. Health 50 (2012) 267–278, https://doi.org/10.2486/indhealth.MS1352.

[100] V.E. Angouridakis, T.J. Makrogiannis, The discomfort-index in thessaloniki, Greece, Int. J. Biometeorol. 26 (1982) 53–59, https://doi.org/10.1007/BF02187617.

[101] E. Jauregui, C. Soto, Wet-bulb temperature and discomfort index areal distribution in Mexico, Int. J. Biometeorol. 11 (1967) 21–28, https://doi.org/10.1007/BF01424271.

[102] S. Conti, P. Meli, G. Minelli, R. Solimini, V. Toccaceli, M. Vichi, C. Beltrano, L. Perini, Epidemiologic study of mortality during the Summer 2003 heat wave in Italy, Environ. Res. 98 (2005) 390–399, https://doi.org/10.1016/j.envres.2004.10.009.

[103] J. Masterson, F. Richardson, Humidex: a Method of Quantifying Human Discomfort Due to Excessive Heat and Humidity, 1979.

[104] J. Orosa, Á. Costa, Effect of climate change on outdoor thermal comfort in humid climates, J. Environ. Health. Sci. Eng. 12 (2014) 46.

[105] D.G.C. Rainham, K.E. Smoyer-Tomic, The role of air pollution in the relationship between a heat stress index and human mortality in Toronto, Environ. Res. 93 (2003) 9–19, https://doi.org/10.1016/S0013-9351(03)00060-4.

[106] C.D. Ashley, C.L. Luecke, S.S. Schwartz, M.Z. Islam, T.E. Bernard, Heat strain at the critical WBGT and the effects of gender, clothing and metabolic rate, Int. J. Ind. Ergon. 38 (2008) 640–644, https://doi.org/10.1016/j.ergon.2008.01.017.

[107] T.E. Bernard, V. Caravello, S.W. Schwartz, C.D. Ashley, WBGT clothing adjustment factors for four clothing ensembles and the effects of metabolic demands, J. Occup. Environ. Hyg. 5 (2007) 1–5, https://doi.org/10.1080/15459620701732355.

[108] A.R. Gaspar, D.A. Quintela, Physical modelling of globe and natural wet bulb temperatures to predict WBGT heat stress index in outdoor environments, Int. J. Biometeorol. 53 (2009) 221–230, https://doi.org/10.1007/s00484-009-0207-6.

[109] D.S. Moran, K.B. Pandolf, Y. Shapiro, Y. Heled, Y. Shani, W.T. Mathew, R. R. Gonzalez, An environmental stress index (ESI) as a substitute for the wet bulb globe temperature (WBGT), J. Therm. Biol. 26 (2001) 427–431, https://doi.org/10.1016/S0306-4565(01)00055-9.

[110] D.S. Moran, K.B. Pandolf, Wet bulb globe temperature (WBGT)–to what extent is GT essential? Aviat Space Environ. Med. 70 (1999) 480–484, https://doi.org/10.1177/1010539510373037.

[111] N.L. Ramanathan, Physiological evaluation of the WBGT index for occupational heat stress, Am. Ind. Hyg. Assoc. J. 34 (1973) 375–383, https://doi.org/10.1080/00028897385068666.

[112] R.R. Gonzalez, Y. Nishi, A.P. Gagge, Experimental evaluation of standard effective temperature a new biometeorological index of man's thermal discomfort, Int. J. Biometeorol. 18 (1974) 1–15, https://doi.org/10.1007/BF01450660.

[113] J. Pickup, R. De Dear, An outdoor thermal comfort index (out - set *) - Part I – the model and its assumptions, in: Biometeorol. Urban Climatol. Turn Millennium. Conf. ICB-ICUC, vol. 99, 2000, pp. 279–283.

[114] G. Ye, C. Yang, Y. Chen, Y. Li, A new approach for measuring predicted mean vote (PMV) and standard effective temperature (SET*), Build. Environ. 38 (2003) 33–44, https://doi.org/10.1016/S0360-1323(02)00027-6.

[115] P. Weihs, H. Staiger, B. Tinz, E. Batchvarova, H. Rieder, L. Vuilleumier, M. Maturilli, G. Jendritzky, The uncertainty of UTCI due to uncertainties in the determination of radiation fluxes derived from measured and observed meteorological data, Int. J. Biometeorol. 56 (2012) 537–555, https://doi.org/10.1007/s00484-011-0416-7.

[116] I. Fato, F. Martellotta, C. Chiancarella, Thermal comfort in the climatic conditions of Southern Italy, ASHRAE Trans. 110 (2004) 578–593.

[117] D. McIntyre, R. Gonzalez, Man's thermal sensitivity during temperature changes at two levels of clothing insulation and activity, ASHRAE Trans. 82 (1976) 219–233.

[118] M.A. Humphreys, J.F. Nicol, Do people like to feel" neutral"? Response to the ASHRAE scale of subjective warmth in relation to thermal preference, indoor and outdoor temperature, ASHRAE Trans. 110 (2004).

[119] J. von Grabe, S. Winter, The correlation between PMV and dissatisfaction on the basis of the ASHRAE and the McIntyre scale – towards an improved concept of dissatisfaction, Indoor Built Environ. 17 (2008) 103–121, https://doi.org/10.1177/1420326X08089364.

[120] I. Holmer, Calculation of predicted mean vote (PMV), and predicted percentage dissatisfied (PPD), JAVA applet ISO 7730. http://www.eat.lth.se/fileadmin/eat/Termisk_miljoe/PMV-PPD.html, 2019.

[121] J. Han, G. Zhang, Q. Zhang, J. Zhang, J. Liu, L. Tian, C. Zheng, J. Hao, J. Lin, Y. Liu, D.J. Moschandreas, Field study on occupants' thermal comfort and residential thermal environment in a hot-humid climate of China, Build. Environ. 42 (2007) 4043–4050, https://doi.org/10.1016/j.buildenv.2006.06.028.

[122] M. Nikolopoulou, N. Baker, K. Steemers, Thermal comfort in outdoor urban spaces: understanding the Human parameter, Sol. Energy 70 (2001) 227–235, https://doi.org/10.1016/S0038-092X(00)00093-1.